JOURNAL OF MAGNETIC RESONANCE **127,** 87–104 (1997)
ARTICLE NO. MN971179

Electron-Spin-Echo Envelope Modulation Arising from Hyperfine Coupling to a Nucleus of Arbitrary Spin

Alessandro Ponti

Centro C.N.R. per lo Studio sulle Relazioni tra Struttura e Reattività Chimica, via Camillo Golgi 19, I-20133 Milan, Italy

Received November 19, 1996; revised April 10, 1997

The electron-spin-echo envelope modulation (ESEEM) arising from hyperfine coupling to a nucleus of arbitrary spin I is investigated. The generic ESEEM pulse sequence, consisting of a succession of nonselective microwave pulses and free-evolution periods, is first considered. It is shown that, when the high-field approximation is valid, the ESEEM for a nucleus of arbitrary spin is a function of the ESEEM for a $I = \frac{1}{2}$ nucleus subject to the same Hamiltonian and that the functional relationship is provided by the Chebyshev polynomials of the second kind. Such relationship also provides a very efficient method for the numerical simulation of the ESEEM due to $I > \frac{1}{2}$ nuclei. Next, the experiments based on the primary and on the stimulated electron-spin-echo pulse sequences are considered and explicit analytical formulas for arbitrary nuclear spin are given. The central result of the theory developed is that the modulation amplitudes are polynomials of degree $2I$ in the modulation depth parameter k. This nonlinearity introduces two differences with respect to the $I = \frac{1}{2}$ case. First, the amplitudes of the fundamental pure and combination modulations, already present for spin-$\frac{1}{2}$ nuclei, are largely nonlinear functions of k; second, harmonics of the fundamental modulations (up to the $2I$th) occur in the ESEEM with amplitudes which can be comparable with those of the fundamentals. As a general rule, nonlinear effects are more important when I is large, provided that all the other factors are the same. Since terms of different order in k alternate in sign, the modulation amplitudes show an oscillating behavior and reach their maximum well before $k = 1$. While the amplitude of the pure modulations is always positive, that of the combination modulations (which occur only in primary and 2-D stimulated ESEEM) can be either positive or negative, depending on the value of k; thence a new type of suppression effect ensues which is independent of interpulse delays. Besides, the well-known suppression effect in the 1-D stimulated ESEEM of $I = \frac{1}{2}$ nuclei occurs also when $I > \frac{1}{2}$ in a similar way. Spectral simulations are presented to illustrate the characteristics of the ESEEM arising from $I > \frac{1}{2}$ nuclei. The theory developed is compared with an earlier analysis which neglected nonlinear terms, and its advantages are demonstrated.

INTRODUCTION

Electron-spin-echo envelope modulation (ESEEM) spectroscopy is a well-established tool for the determination of the electronic and geometric structure of paramagnetic sites through the measurement of nuclear transition frequencies. It is especially useful in the investigation of solid samples which often feature poorly resolved inhomogeneously broadened spectra in the conventional electron paramagnetic resonance experiment (*1*).

The envelope modulation of the primary (two-pulse) electron spin echo, first observed in 1961 by Mims *et al.* (*2*), was theoretically described a few years later (*3*). A spin system with arbitrary electron and nuclear spin quantum numbers (S and I, respectively) was considered and a general recipe for the calculation of the ESEEM was reported which, however, neglected the nuclear quadrupole interaction. The explicit ESEEM formula was obtained for the special case $S = \frac{1}{2}$, $I = \frac{1}{2}$. Later, there was proposed another general scheme (*4*) for the calculation of ESEEM based on the matrix representation of operators. In this way, explicit formulas for the primary and for the stimulated (three-pulse) ESEEM were obtained for a spin system consisting of one electron and one nucleus with $I = \frac{1}{2}$ or 1. In the latter case, the nuclear quadrupole interaction was treated as a small perturbation affecting only the nuclear transition frequencies. The problem of computing the ESEEM due to a nucleus of arbitrary spin was also considered, but an explicit formula was obtained only by neglecting the nuclear quadrupole interaction and by assuming that the modulation is very shallow (*5*). It is worthwhile to point out how the adjective ''explicit'' is meant. Such formulas can be said to be explicit because the echo amplitude is expressed as a linear combination of cosine functions, their arguments containing the modulation frequencies and the time intervals between the pulses and their amplitudes being proportional to a single parameter, namely the modulation depth parameter k. On one hand, this parameter has a clear physical (and even geometrical) interpretation and is readily related to the strength of the nuclear magnetic interactions; on the other hand, the echo-modulation amplitude is completely determined by k and I. Thus, the modulation-depth parameter is a theoretical tool which permits a thorough examination and comparison of the amplitude of the various echo modulations as a function

1090-7807/97 $25.00

of a single parameter, without reference to particular values of the spin Hamiltonian parameters.

Of course, explicit formulas transparently describe either the time-domain ESEEM or the frequency-domain spectrum since the Fourier transformation which relates them is trivial. Explicit ESEEM formulas can be found in the literature almost exclusively for the $S = \frac{1}{2}$, $I = \frac{1}{2}$ system, which has been employed as a model system for the theoretical description of new ESEEM experiments. Attention has been devoted to include the effect of the nuclear quadrupole interaction on the modulation amplitude in the $S = \frac{1}{2}$, $I = 1$ system, and results at different approximation levels have been obtained (*6–9*). More recently, the $I = \frac{5}{2}$ case (*10, 11*) has also been considered. However, no explicit ESEEM formula has been reported: in any case, the modulation amplitude was given as a rather complicated expression involving many matrix elements of the quantum propagators related to the pulse sequence considered.

The aim of this work is to investigate the relationship among the ESEEM arising from hyperfine coupling to nuclei of unequal spin and to calculate the explicit expression for the primary and the stimulated ESEEM due to a nucleus of arbitrary spin. The scope of the present paper is restricted to standard ESEEM experiments which involve only nonselective microwave pulses. Recently, experiments have been proposed which make use of selective (*12*), semi-selective (*13*), or matched (*14*) excitation. Such advanced experiments improve the standard experiments in several respects; nevertheless, the latter are still the most widely used in application work.

In Ref. (*3*), it was already shown that, omitting the nuclear quadrupole interaction, the ESEEM is the trace of a $(2I + 1)$-dimensional rotation matrix but it was Dikanov *et al.* (*15*) who exploited this algebraic property of the ESEEM to demonstrate that the primary and the stimulated ESEEM due to a nucleus of arbitrary spin can be written as a polynomial in which the independent variable is the ESEEM due to a hypothetical $I = \frac{1}{2}$ nucleus subject to the same interactions as the real one. However, they did not find the polynomial coefficients and thus they could not calculate explicit ESEEM formulas. In this paper, it is proved that, when the high-field approximation is valid and the quadrupole interaction is neglected, such a polynomial relationship exists for any standard ESEEM experiment and that the polynomials are the Chebyshev polynomials of the second kind. These results are used to calculate explicit formulas for the primary and the stimulated ESEEM arising from hyperfine coupling to a nucleus of arbitrary spin. Such formulas are based on the same approximations and have the same validity as the well-known expressions for the $S = \frac{1}{2}$, $I = \frac{1}{2}$ spin system. They show that, when the nuclear spin is larger than $\frac{1}{2}$, the ESEEM amplitude depends on the modulation depth parameter k in a largely nonlinear way. This behavior causes many new facets of ESEEM spectroscopy to come to light.

The nuclear quadrupole interaction cannot be taken into account rigorously since, because the quadrupole Hamiltonian is quadratic in the nuclear spin operators, the associated propagator is not a rotation matrix in the nuclear spin space, an indispensable requisite, as we will see, for the theoretical treatment presented. Since every $I > \frac{1}{2}$ nucleus possesses a nuclear quadrupole moment, the question arises as to which nuclei are amenable to this theory. Among these, there are certainly nuclei with such a small nuclear quadrupole *moment* that the nuclear quadrupole *interaction* can be very often neglected, e.g., ^{2}H ($I = 1$) (*16*) and ^{133}Cs ($I = \frac{7}{2}$) (*17*). However, as the nuclear quadrupole interaction depends also on the microscopic environment through the electric field gradient at the nucleus, several cases have been reported where the ESEEM is only slightly affected by the nuclear quadrupole *interaction* despite a rather large nuclear quadrupole *moment*, e.g., ^{7}Li ($I = \frac{3}{2}$) in the lithium-compensated Ti^{3+} center in α quartz (*18*), ^{17}O ($I = \frac{5}{2}$) in the hexaaquomanganese(II) complex (*19*), and even ^{35}Cl and ^{37}Cl ($I = \frac{3}{2}$) in the IV coordination shell of the F center in KCl (*20*). In such cases, the effect of the nuclear quadrupole interaction reduces to a broadening and/or splitting of the frequency-domain peaks, but the center frequency and the total amplitude of the resulting multiplet are those predicted neglecting the nuclear quadrupole interaction (*4, 16b*). In any case, even when the nuclear quadrupole interaction is large, the simplification introduced by ignoring the quadrupole term is so considerable that it may be worth approximating in this way in order to obtain an estimate of the amplitude of the modulations (*5*).

The paper is structured as follows. First, the theoretical background of ESEEM spectroscopy is briefly reviewed and the approximations involved are clearly stated. Second, it is shown that the ESEEM due to nuclei with different spin are related to each other by the Chebyshev polynomials of the second kind and the explicit primary and stimulated ESEEM formulae for arbitrary I are derived. Next, the modulation amplitudes are analyzed and the differences between the $I = \frac{1}{2}$ and the $I > \frac{1}{2}$ cases are described and illustrated by spectral simulations. Finally, the main results of the present work are summarized.

THEORETICAL BACKGROUND

The theory of ESEEM has been reported many times (*3, 4, 21, 22*); therefore in this section, I report only the main features of the model system and summarize the matrix method used to compute the evolution of spin systems under time-independent Hamiltonian operators, also showing the approximations involved.

The present paper deals with a spin system consisting of one electron with spin $S = \frac{1}{2}$ and one nucleus with arbitrary spin I placed in a uniform magnetic field $\mathbf{B}_0$ which defines

the z axis of the laboratory reference frame. The spins are coupled to $\mathbf{B}_0$ by the Zeeman interaction and to each other by the hyperfine interaction. In the usual frame rotating about the z axis at the microwave frequency the Hamiltonian operator in angular units is

$$H_0 = \Omega_S S_z + \omega_I I_z + A S_z I_z + B S_z I_x, \quad [1]$$

where $\Omega_S = g\beta B_0/\hbar - \omega_{\mathrm{mw}}$ is the offset from the microwave frequency ω_{mw}, $\omega_I = g_I \beta_n B_0/\hbar$ is the nuclear Larmor frequency, and A and B are related to the elements of the hyperfine matrix $\mathbf{A}$ in the laboratory frame:

$$A = A_{zz},\ B = \sqrt{A_{zx}^2 + A_{zy}^2}. \quad [2]$$

There are three assumptions underlying Eq. [1], i.e., that the electron and nuclear Zeeman interactions are isotropic and that the former is much larger then the hyperfine interaction (high-field approximation). The Hamiltonian H_0 is not diagonal with respect to the nuclear spin because of the anisotropy of the hyperfine interaction which makes the effective field at the nucleus—and then the quantization axis of the nuclear spin—not parallel to $\mathbf{B}_0$. The effective field depends on the electron spin state both in magnitude and in direction, that is, both the nuclear sublevel energy and the orientation of the nuclear quantization axis depend on m_S. The eigenvalues of H_0 are

$$E(m_S, m_I) = m_S \Omega_S + m_I \sqrt{(\omega_I + m_S A)^2 + (m_S B)^2}, \quad [3]$$

where the square root represents the nuclear transition frequencies ω_α and ω_β in the $m_S = +\frac{1}{2}$ and $-\frac{1}{2}$ manifold, respectively. The effective-field vectors at the nucleus in the two m_S manifolds define the angle

$$2\eta = \arctan \frac{B}{A + 2\omega_I} - \arctan \frac{B}{A - 2\omega_I}, \quad [4]$$

which plays a fundamental role in ESEEM spectroscopy. In fact, the modulation depth parameter is $k = \sin^2 2\eta$ ($0 \leqslant k \leqslant 1$). To observe the echo modulation, it is then necessary that $B \neq 0$, i.e., that the hyperfine interaction is anisotropic. One expects a small k when the nuclear Zeeman interaction predominates over the hyperfine interaction or vice versa, since then $\eta \cong 0$ or $\eta \cong \pi/2$. On the other hand, a large k is expected when the two interactions have approximately the same strength since then $2\omega_I \cong (A^2 + B^2)^{1/2}$ and $\eta \cong \pi/4$.

A quantum spin system is completely defined by its density operator $\boldsymbol{\sigma}$, as the expectation value of any physical quantity can be computed as

$$\langle \mathrm{Op} \rangle = \mathrm{Tr}\{\boldsymbol{\sigma} \mathrm{Op}\} \quad [5]$$

where Op is the operator associated with the quantity and Tr is the trace. In the present paper, all quantum operators are represented by square matrices of dimension $2(2I + 1)$ equal to the number of states of the spin system, and the simple products $|m_S, m_I\rangle$ of the eigenfunctions of S_z and I_z are used as basis functions. The high-field approximation suggests partitioning such matrices with respect to the electron spin S since m_S is a good quantum number. In the following, I write them as 2×2 matrices, the elements of which are matrices defined in the $(2I + 1)$-dimensional Hilbert subspace associated with the nuclear spin (I space). The density matrix is then written as

$$\boldsymbol{\sigma} = \begin{bmatrix} \sigma_{\alpha\alpha} & \sigma_{\alpha\beta} \\ \sigma_{\beta\alpha} & \sigma_{\beta\beta} \end{bmatrix} \quad [6]$$

The four blocks can be classified as to the electron coherence order (*23*), i.e., the difference in m_S between the states connected by each block. The off-diagonal blocks $\sigma_{\alpha\beta}$ and $\sigma_{\beta\alpha}$ connect states in different m_S manifolds, and then their electron coherence order is, respectively, $+1$ and -1. The diagonal blocks $\sigma_{\alpha\alpha}$ and $\sigma_{\beta\beta}$ connect states within the same m_S manifold, and both have zero electron coherence order.

At the beginning of experiments, the sample is in thermal equilibrium at temperature T and, assuming that the spin Hamiltonian H_0 is much smaller than the thermal energy kT (high-temperature approximation), the initial density matrix $\boldsymbol{\sigma}(0)$ can be written as

$$\boldsymbol{\sigma}(0) \cong -S_z = -\frac{1}{2} \begin{bmatrix} 1_I & 0_I \\ 0_I & -1_I \end{bmatrix}, \quad [7]$$

where 1_I and 0_I are the identity (unit) and null (zero) matrices of dimension $(2I + 1)$, and constant terms are neglected. The time evolution of the spin system is governed by the Liouville equation

$$\frac{d}{dt} \boldsymbol{\sigma}(t) = -i[H, \boldsymbol{\sigma}(t)] \quad [8]$$

where H is the spin Hamiltonian operator and relaxation is neglected. Any ESEEM experiment is based on a pulse sequence, that is, on a succession of microwave pulses and free-evolution periods during which the system is subject to different but constant Hamiltonian operators $H_1, H_2, \ldots, H_n$. The density operator at the end of the experiment is

$$\boldsymbol{\sigma}(t_1 + \cdots + t_n) = e^{-iH_n t_n} \cdots e^{-iH_1 t_1} \boldsymbol{\sigma}(0) e^{iH_1 t_1} \cdots e^{iH_n t_n}. \quad [9]$$

During a free-evolution period of duration t, the spin system is subject to H_0, and the corresponding propagator is

$$\exp(-iH_0t) = \begin{bmatrix} \exp(-iH_\alpha t) & 0 \\ 0 & \exp(-iH_\beta t) \end{bmatrix}, \quad [10]$$

where H_α and H_β are reduced Hamiltonian operators in the $m_S = +\frac{1}{2}$ and $m_S = -\frac{1}{2}$ manifold, respectively, which can be written as

$$\left.\begin{matrix} H_\alpha \\ H_\beta \end{matrix}\right\} = \pm(\Omega_S/2)1_I + (\omega_I \pm A/2)I_z \pm (B/2)I_x$$

$$= \begin{cases} +(\Omega_S/2)1_I + J_\alpha \\ -(\Omega_S/2)1_I + J_\beta \end{cases}, \quad [11]$$

where J_α and J_β are angular momentum operators which describe the interaction of the nuclear spin with the effective field in the $m_S = +\frac{1}{2}$ and $-\frac{1}{2}$ manifold, respectively. During microwave pulses, the system is subject to the rotating frame Hamiltonian

$$H = H_0 + H_p = H_0 + \omega_1 S_y, \quad [12]$$

where ω_1 is the strength of the component of the microwave field which is static in the rotating frame.

The description of the evolution during microwave pulses is greatly simplified if it is assumed that H_p is much larger than H_0. The pulse is then said to be ideal or nonselective since it excites uniformly all spin packets which constitute the EPR spectrum. The ideal-pulse approximation is formally stated by writing the propagator for a nonselective pulse directed along the y axis of the rotating frame as

$$\exp(-i\beta S_y) = \begin{bmatrix} \cos\left(\frac{\beta}{2}\right)1_I & -\sin\left(\frac{\beta}{2}\right)1_I \\ \sin\left(\frac{\beta}{2}\right)1_I & \cos\left(\frac{\beta}{2}\right)1_I \end{bmatrix}, \quad [13]$$

where β is the pulse turning angle. The evolution of the density matrix during a given pulse sequence is computed by these propagators.

At the end of the sequence, the echo is detected 90° off-phase from the microwave pulses at time t_{echo}. The contribution of a single spin packet to the echo amplitude is computed as the expectation value of S_x

$$\langle S_x \rangle \equiv \text{Tr}\{\boldsymbol{\sigma}(t_{\text{echo}})S_x\} = \text{Re Tr}\{\sigma_{\alpha\beta}(t_{\text{echo}})\} \quad [14]$$

since $\boldsymbol{\sigma}$ is hermitian and then $\sigma_{\beta\alpha} = \sigma^\dagger_{\alpha\beta}$. Summing over all the spin packets yields the echo amplitude

$$E(t_{\text{echo}}) \equiv \overline{\langle S_x \rangle} = \int_{-\infty}^{+\infty} \text{Re Tr}\{\sigma_{\alpha\beta}(t_{\text{echo}})\}g(\Omega_S)d\Omega_S, \quad [15]$$

where $g(\Omega_S)$ is the normalized shape of the absorption EPR spectrum. In ESEEM spectroscopy, it is customary to normalize the echo by the amplitude $E(0)$ of the echo when all time intervals are zero. The normalized ESEEM is then defined as

$$M = E(t_{\text{echo}})/E(0). \quad [16]$$

ESEEM DUE TO A NUCLEUS OF ARBITRARY SPIN

General Properties of ESEEM

In this subsection, I demonstrate that a close link exists between the ESEEM arising from nuclei of unequal spin whenever the high-field approximation is valid. As a first step, I prove that each block in the density matrix always consists of a linear combination of rotation matrices acting in I space. Second, I find the relationship between the ESEEM $M(I)$ stemming from different I values using some results from the group theory of rotations.

At the beginning of ESEEM experiments, electron coherence is created by applying to the sample in thermal equilibrium a nonselective $\pi/2$ pulse which can be assumed to be along the y axis of the rotating frame. Using Eqs. [7], [9], and [13], the density matrix after the pulse can be written as

$$\boldsymbol{\sigma}(0^+) = -\frac{1}{2}\begin{bmatrix} 0_I & 1_I \\ 1_I & 0_I \end{bmatrix}. \quad [17]$$

The off-diagonal blocks are the identity matrix in I space, which is the (trivial) rotation matrix through a null angle. During the experiment, the density matrix undergoes changes caused either by nonselective pulses or by free evolution. Without fixing attention on a particular sequence, I consider the effect of a free-evolution period of duration t on the generic density matrix $\boldsymbol{\sigma}$. From Eqs. [6], [9], [10], and [11], one can write

$$e^{-iH_0t}\boldsymbol{\sigma}e^{iH_0t} = \begin{bmatrix} e^{-iJ_\alpha t}\sigma_{\alpha\alpha}e^{iJ_\alpha t} & e^{-i\Omega_S t}e^{-iJ_\alpha t}\sigma_{\alpha\beta}e^{iJ_\beta t} \\ e^{i\Omega_S t}e^{-iJ_\beta t}\sigma_{\beta\alpha}e^{iJ_\alpha t} & e^{-iJ_\beta t}\sigma_{\beta\beta}e^{iJ_\beta t} \end{bmatrix}. \quad [18]$$

Since the J_μ ($\mu = \alpha, \beta$) are nuclear angular momentum operators, the exponential matrices $\exp(\pm iJ_\mu t)$ are rotation matrices in I space. Of course, the product of two or more rotation matrices is another rotation matrix acting in the same space, and then the transformed blocks of σ are rotation matrices in the I space. For instance, the off-diagonal blocks

of $\boldsymbol{\sigma}(0^+)$ transform into other rotation matrices while the diagonal blocks remain null. Note that the free evolution makes the $\sigma_{\mu\nu}$ block (μ, $\nu = \alpha$, β) left-multiplied by $\exp(-iJ_\mu t)$ and right-multiplied by $\exp(iJ_\nu t)$ so that the evolution history of each part of the density matrix is recorded in the free-evolution propagators. Moreover, the off-diagonal blocks are multiplied by the appropriate phase factor $\exp(\pm i\Omega_S t)$ which accounts for the dephasing of the electron spins.

The effect on the generic density matrix $\boldsymbol{\sigma}$ of an ideal pulse along the y axis of the rotating frame with turning angle β is given by

$$e^{-i\beta S_y}\boldsymbol{\sigma}e^{i\beta S_y} = \begin{bmatrix} c^2\sigma_{\alpha\alpha} + s^2\sigma_{\beta\beta} - sc(\sigma_{\alpha\beta} + \sigma_{\beta\alpha}) & c^2\sigma_{\alpha\beta} - s^2\sigma_{\beta\alpha} + sc(\sigma_{\alpha\alpha} - \sigma_{\beta\beta}) \\ c^2\sigma_{\beta\alpha} - s^2\sigma_{\alpha\beta} + sc(\sigma_{\alpha\alpha} - \sigma_{\beta\beta}) & c^2\sigma_{\beta\beta} + s^2\sigma_{\alpha\alpha} + sc(\sigma_{\alpha\beta} + \sigma_{\beta\alpha}) \end{bmatrix}, \quad [19]$$

where $c = \cos(\beta/2)$ and $s = \sin(\beta/2)$. The pulse causes transfers among the different blocks. In particular, a π pulse ($c = 0$, $s = 1$) exchanges $\sigma_{\alpha\alpha}$ with $\sigma_{\beta\beta}$ and $\sigma_{\alpha\beta}$ with $\sigma_{\beta\alpha}$, whereas after a $\pi/2$ pulse ($c = s = 2^{-1/2}$), each block is a linear combination of all the four blocks of the density matrix before the pulse. Again, if the original blocks are linear combinations of rotation matrices in I space, the transformed blocks are also linear combinations of rotation matrices in the same space. It is then proved that, throughout an ESEEM experiment, the off-diagonal blocks are linear combinations of rotation matrices defined in I space. As for the diagonal blocks, they remain null if there are only π pulses in addition to the initial $\pi/2$ pulse (as in primary ESEEM); if there is at least another pulse with turning angle $\beta \neq \pi$ in addition to the first pulse, the diagonal blocks are also linear combinations of rotation matrices in I space because of transfer from the off-diagonal blocks. If microwave pulses with arbitrary phase are used, there are additional constant phase factors but the proof remains valid. In this case, however, the electron spin echo is no longer directed along the x axis of the rotating frame. The rules to predict the direction of the echo can be found elsewhere (*24*).

Consider now a generic ESEEM pulse sequence consisting of r nonselective pulses and r free-evolution periods of duration τ_j ($j = 1, 2, \ldots, r$), as depicted in Fig. 1a. The amplitude of the echo occurring at $t_{\text{echo}} = \Sigma_{j=1}^{r} \tau_j$ is monitored during the experiment. Recalling the preceding discussion, one can write the upper-right block of the density matrix at echo time $\sigma_{\alpha\beta}(t_{\text{echo}})$ as a sum over all the rotation matrices $G_n(I)$ generated by the pulse sequence

$$\sigma_{\alpha\beta}(t_{\text{echo}}) = \frac{1}{2}\sum_n c_n e^{-i\Omega_S t_n} G_n(I). \quad [20]$$

The c_n are real coefficients which depend only on the turning angle and phase of the pulses, and the overall factor $\frac{1}{2}$ is for future convenience. Each $G_n(I)$ is a product of exponential matrices involving J_α and J_β and represents one of the possible coherence-transfer pathways contributing to the echo amplitude. As already pointed out, the pathway is recorded in the sequence of the exponential matrices which appear in the $G_n(I)$ itself. The exponential phase factors contain the linear combinations $t_n = \Sigma_{j=1}^{r} h_j^{(n)}\tau_j$ of the time intervals τ_j between pulses, where the coefficients $h_j^{(n)}$ are the electron coherence order during interval τ_j of that part of the density matrix which gives rise to $G_n(I)$.

Using Eqs. [15] and [20], one can write the normalized ESEEM due to a nucleus of spin I as

$$\begin{aligned} M(I) = \frac{E(t_{\text{echo}})}{E(0)} &= \frac{2}{2I+1} \\ &\times \int_{-\infty}^{+\infty} \text{Re Tr}\left\{\frac{1}{2}\sum_n c_n e^{-i\Omega_S t_n} G_n(I)\right\} g(\Omega_S)\, d\Omega_S \\ &= \frac{1}{2I+1} \\ &\times \text{Re Tr}\left\{\sum_n c_n G_n(I) \int_{-\infty}^{+\infty} e^{-i\Omega_S t_n} g(\Omega_S)\, d\Omega_S\right\} \quad [21] \end{aligned}$$

since $E(0) = (2I + 1)/2$. When $t_n = 0$, the integral amounts to 1 and the corresponding $G_n(I)$ contributes to the echo. When $t_n \neq 0$, the integral is zero because the range of $\Omega_S t_n$ is much larger than 2π. Physically, this means that the electron spins are uniformly spread in the x, y plane, and the corresponding $G_n(I)$ does not contribute to the echo. Restricting the summation to the $G_n(I)$ which do not vanish upon integration, the normalized ESEEM becomes

$$\begin{aligned} M(I) &= \frac{1}{2I+1}\,\text{Re}\sum_n c_n \text{Tr}\{G_n(I)\} \\ &= \text{Re}\sum_n c_n V_n(I), \quad [22] \end{aligned}$$

where $V_n(I) = \text{Tr}\{G_n(I)\}/(2I + 1)$ is that part of the ESEEM which stems from the electron coherence-transfer pathway represented by $G_n(I)$. The group theory of rotations (*25, 26*) states that every rotation matrix $G_n(I)$ in I space belongs to the $(2I + 1)$-dimensional irreducible representation of the $SU(2)$ group of the unitary unimodular matrices. Hence, the trace of $G_n(I)$ is the (real) character of a rotation in a $(2I + 1)$-dimensional space, and the last expression can be written as

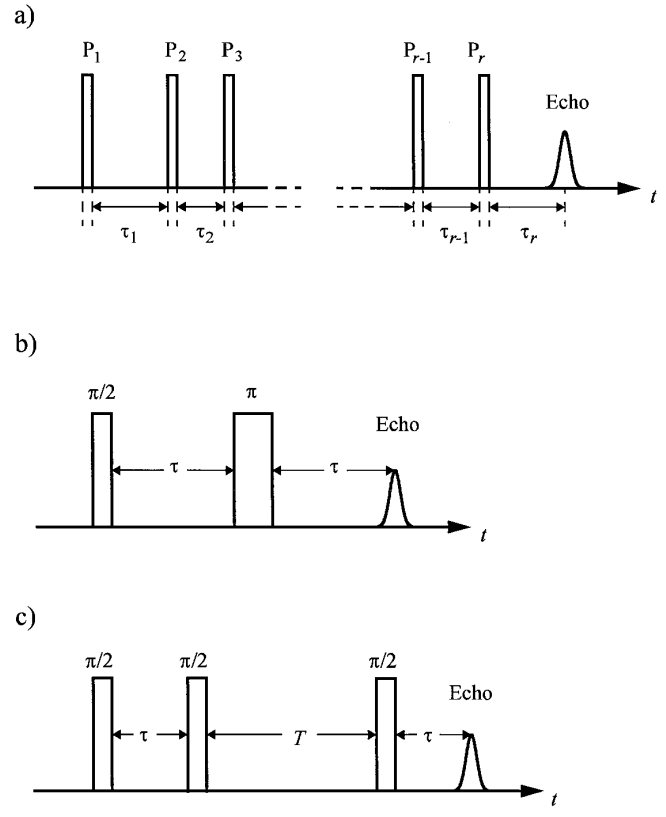

FIG. 1. Pulse sequences for ESEEM experiments. (a) Generic experiment, (b) primary ESEEM, (c) stimulated ESEEM.

$$M(I) = \sum_n c_n V_n(I),$$

$$V_n(I) = \frac{1}{2I+1}\,\frac{\sin[(2I+1)\xi_n]}{\sin\xi_n}. \qquad [23]$$

The real parameters ξ_n can be determined (*15*) by substituting $I = \frac{1}{2}$ in the last equation:

$$V_n(1/2) = \cos\xi_n. \qquad [24]$$

The last two equations implicitly tell us that $V_n(I)$ is a polynomial of degree $2I$ in $V_n(\frac{1}{2})$. However, such expressions do not allow one to go further in a general way. To do so, we need to find an explicit expression of the relationship between $V_n(I)$ and $V_n(\frac{1}{2})$. The Chebyshev polynomials of the second kind (*27, 28*)

$$U_{2I}(x) = \sum_{q=0}^{[I]} (-1)^q \binom{2I-q}{q} (2x)^{2(I-q)},$$

$$\binom{2I-q}{q} = \frac{(2I-q)!}{q!(2I-2q)!}, \qquad [25]$$

where $[I]$ is the largest integer not greater than I (the square brackets have this meaning only when they appear in a summation limit), fulfill the condition

$$U_{2I}(\cos\xi_n) = \frac{\sin[(2I+1)\xi_n]}{\sin\xi_n},$$

$$I = 0, \tfrac{1}{2}, 1, \tfrac{3}{2}, \ldots. \qquad [26]$$

Substituting $\cos\xi_n = V_n(\frac{1}{2})$ in Eq. [26] and using Eq. [23], it is found that

$$V_n(I) = \frac{1}{2I+1}\,U_{2I}[V_n(\tfrac{1}{2})]. \qquad [27]$$

It is thus proved that, when the high-field approximation is valid, $V_n(I)$ can be easily calculated from $V_n(\frac{1}{2})$ by means of the Chebyshev polynomials of the second kind. The complete ESEEM formula is readily obtained by summing the contributions from all the coherence-transfer pathways, as given in Eq. [23]. The $U_{2I}(x)$ relevant to ESEEM spectroscopy are reported in Table 1.

Explicit ESEEM Formulas

The results of the previous subsection are now used to calculate the explicit analytical formulas for the ESEEM arising from hyperfine coupling to a nucleus of arbitrary spin. From now on, the two-pulse ($\pi/2$—τ—π—τ) and the three-pulse ($\pi/2$—τ—$\pi/2$—T—$\pi/2$—τ) sequences, which are reported in Figs. 1b, c, are considered. ESEEM experiments result from the combination of a pulse sequence with an incrementation scheme, but the analytical formula of the ESEEM depends only on the pulse sequence and then it applies to any experiment based on that sequence. While primary ESEEM (*3, 4*) is the only experiment derived from

TABLE 1
Chebyshev Polynomials of the Second Kind $U_{2I}(x)$

I	$U_{2I}(x)$
0	1
$\frac{1}{2}$	$2x$
1	$4x^2 - 1$
$\frac{3}{2}$	$8x^3 - 4x$
2	$16x^4 - 12x^2 + 1$
$\frac{5}{2}$	$32x^5 - 32x^3 + 6x$
3	$64x^6 - 80x^4 + 24x^2 - 1$
$\frac{7}{2}$	$128x^7 - 192x^5 + 80x^3 - 8x$
4	$256x^8 - 448x^6 + 240x^4 - 40x^2 + 1$
$\frac{9}{2}$	$512x^9 - 1024x^7 + 672x^5 - 160x^3 + 10x$
5	$1024x^{10} - 2304x^8 + 1792x^6 - 560x^4 + 61x^2 - 1$
$\frac{11}{2}$	$2048x^{11} - 5120x^9 + 4608x^7 - 1792x^5 + 280x^3 - 12x$
6	$4096x^{12} - 11264x^{10} + 11520x^8 - 5376x^6 + 1120x^4 - 84x^2 + 1$

the two-pulse sequence, two experiments are based on the three-pulse sequence: 1-D stimulated ESEEM (*4, 29*) ($\tau' \equiv \tau + T$ incremented) and 2-D stimulated ESEEM (*30*) (τ and τ' independently incremented). To predict and to interpret the results of the various experiments based on the same sequence, it is often advisable to simplify the general formula by showing only the time intervals which are varied during the experiment. In the following, we will see an example of such a procedure applied to stimulated ESEEM.

Following the previously discussed procedure, the r-pulse ESE modulation $M_r(I)$ ($r = 2, 3$) for a nucleus of spin I can be easily worked out as

$$M_2(I) = V_2(I),\ G_2(I) = e^{-iJ_\alpha\tau}e^{-iJ_\beta\tau}e^{iJ_\alpha\tau}e^{iJ_\beta\tau} \quad [28]$$

$$M_3(I) = \tfrac{1}{2}[V_{3\alpha}(I) + V_{3\beta}(I)],$$

$$G_{3\alpha}(I) = e^{-iJ_\alpha\tau'}e^{-iJ_\beta\tau}e^{iJ_\alpha\tau'}e^{iJ_\beta\tau},$$

$$G_{3\beta}(I) = e^{-iJ_\alpha\tau}e^{-iJ_\beta\tau'}e^{iJ_\alpha\tau}e^{iJ_\beta\tau'}, \quad [29]$$

where mnemonic subscripts are used for the $V_n(I)$ and the $G_n(I)$. $G_2(I)$ represents electron coherence which evolved in $\sigma_{\beta\alpha}$ during the first evolution period and in $\sigma_{\alpha\beta}$ during the second one. Either $G_{3\alpha}(I)$ or $G_{3\beta}(I)$ represents the parts of the density matrix that evolved as electron coherence in $\sigma_{\beta\alpha}$ during the first evolution period and in $\sigma_{\alpha\beta}$ during the third, but that dwelled in $\sigma_{\alpha\alpha}$ and in $\sigma_{\beta\beta}$, respectively, during $T = \tau' - \tau$. These examples show that the partition of the ESEEM into the $V_n(I)$ is unique and based on physical grounds. To compute the $V_n(I)$, there are needed the well-known explicit expressions of the $V_n(\frac{1}{2})$ for the primary echo modulation (*3, 4*)

$$V_2(\tfrac{1}{2}) = 1 - k[\tfrac{1}{2}(1 - \cos\omega_\alpha\tau)(1 - \cos\omega_\beta\tau)] \quad [30]$$

and for the stimulated echo modulation (*4, 30*)

$$V_{3\alpha}(\tfrac{1}{2}) = 1 - k[\tfrac{1}{2}(1 - \cos\omega_\alpha\tau')(1 - \cos\omega_\beta\tau)]. \quad [31]$$

$V_{3\beta}$ can be obtained from $V_{3\alpha}$ by exchanging α and β everywhere.

The above developed theory implies that when $I > \frac{1}{2}$ the ESEEM amplitude depends nonlinearly on the modulation depth parameter k. Now k is introduced in order to divide $V_n(I)$ into terms linear, quadratic, cubic, etc., in k. For the pulse sequences considered, one can rewrite $V_n(\frac{1}{2})$ as

$$V_n(\tfrac{1}{2}) = 1 - kW_n, \quad [32]$$

where W_n contains the nuclear transition frequencies and does not depend on k. Substituting Eq. [32] in Eq. [27], using the binomial theorem and rearranging the sum, one obtains

$$V_n(I) = \sum_{p=0}^{2I} C_p(I)k^pW_n^p, \quad [33]$$

where

$$C_p(I) = \sum_{q=0}^{[(2I-p)/2]} (-1)^{p+q}\frac{2^{2I-2q}}{2I+1}\binom{2I-q}{q}\binom{2I-2q}{p}. \quad [34]$$

To compute this summation, notice that $C_p(I)$ is proportional to the pth derivative of $U_{2I}(x)$ evaluated at $x = 1$:

$$C_p(I) = \frac{1}{2I+1}\frac{(-1)^p}{p!}U_{2I}^{(p)}(1). \quad [35]$$

This intermediate result makes it possible to find a very simple expression for $C_p(I)$ since the $U_{2I}(x)$ are the solutions of the Chebyshev equation of the second kind (*28*)

$$(1 - x^2)U_{2I}^{(2)}(x) - 3xU_{2I}^{(1)}(x) + 2I(2I + 2)U_{2I}(x) = 0, \quad [36]$$

valid for $-1 \leqslant x \leqslant +1$. Evaluating Eq. [36] at $x = 1$ and noting that $U_{2I}(1) = 2I + 1$, one obtains

$$U_{2I}^{(1)}(1) = \frac{1}{3}(2I + 2)(2I + 1)(2I). \quad [37]$$

The higher derivatives are obtained by further differentiating Eq. [36] with respect to x and substituting $x = 1$. The general expression is readily recognized to be

$$U_{2I}^{(p)}(1) = \frac{(2I + 1 + p)(2I + p)\ldots(2I + 1 - p)}{1\cdot3\cdot5\cdot\ldots\cdot(2p + 1)} = \frac{(2I + 1 + p)!}{(2I - p)!(2p + 1)!!}, \quad [38]$$

where $(2p + 1)!!$ is the double factorial of $2p + 1$, i.e., the product of the odd natural numbers up to $2p + 1$. $C_p(I)$ can now be expressed as a rational number by merging Eqs. [35] and [38] into the expression

$$C_p(I) = \frac{1}{2I + 1}\frac{(-1)^p(2I + 1 + p)!}{p!(2I - p)!(2p + 1)!!}. \quad [39]$$

Special cases are $C_0(I) = 1$ and $C_1(I) = -(\frac{4}{3})I(I + 1)$.

The coefficients of the polynomial in Eq. [33] contain only the nuclear spin I in addition to the dummy index p. The expressions developed up to now are valid for any ESEEM experiment for which one can write Eqs. [27] and [32].

In order to work out the analytical formulas for the ESEEM, we consider the generic term W_n^p and transform it in a linear combination of cosine functions, where the arguments contain the modulation frequencies that one finds in the ESEEM. Then all the W_n^p are summed so that $V_n(I)$ is expressed as a weighted sum over all possible modulations. Finally, the ESEEM $M_r(I)$ is computed as a summation, the coefficients of which represent the amplitude of the peaks in the Fourier-transformed ESEEM spectrum.

To keep notation at a minimum, W_n is rewritten as

$$W_n = \tfrac{1}{2}(1 - \cos\alpha)(1 - \cos\beta) \qquad [40]$$

for $n = 2, 3\alpha, 3\beta$. The arguments α and β, proportional to the nuclear transition frequencies ω_α and ω_β, can be identified by comparison with Eqs. [30] and [31]. The algebraic similarity between primary and stimulated ESEEM can be traced back to the fact that primary ESEEM can be formally considered as a special case of stimulated ESEEM obtained by setting $T = 0$. Using the binomial theorem, one can write

$$W_n^p = 2^{-p}\left[\sum_{q=0}^{p}(-1)^q\binom{p}{q}\cos^q\alpha\right] \times\left[\sum_{q'=0}^{p}(-1)^{q'}\binom{p}{q'}\cos^{q'}\beta\right]. \qquad [41]$$

Now we use the formula (*31*) which gives $\cos^q\alpha$ as a sum of cosines of multiples of α

$$\cos^q\alpha = 2^{1-q}\sum_{m=0}^{[q/2]}\epsilon(q-2m)\binom{q}{m}\cos[(q-2m)\alpha],$$

$$\epsilon(x) = \begin{cases} 1/2 & \text{if } x = 0 \\ 1 & \text{otherwise} \end{cases} \qquad [42]$$

to show which modulations arise from the single power under consideration. The first summation in square brackets in Eq. [41] becomes

$$\sum_{q=0}^{p}\sum_{m=0}^{[q/2]}(-1)^q 2^{1-q}\binom{p}{q}\binom{q}{m} \times\epsilon(q-2m)\cos[(q-2m)\alpha]. \qquad [43]$$

We now rearrange the last expression so that one of the summations runs explicitly over the modulation index $n_\alpha \equiv q - 2m$. To do so, a cascade of transformations must be carefully applied to both indexes q and m, and the last expression becomes

$$\sum_{n_\alpha=0}^{p}\sum_{m=0}^{[(p-n_\alpha)/2]}(-1)^{n_\alpha}2^{1-(2m+n_\alpha)}\binom{p}{2m+n_\alpha} \times\binom{2m+n_\alpha}{m}\epsilon(n_\alpha)\cos(n_\alpha\alpha). \qquad [44]$$

Processing in the same manner the summation involving $\cos^{q'}\beta$ and defining n_β similarly to n_α, one can write, after some rearrangements,

$$W_n^p = 2^{-p}\sum_{n_\alpha=0}^{p}\sum_{n_\beta=0}^{p}Q_p(n_\alpha)Q_p(n_\beta)\cos(n_\alpha\alpha)\cos(n_\beta\beta), \qquad [45]$$

where

$$Q_p(n) = (-1)^n 2^{1-n}\epsilon(n) \times\sum_{m=0}^{[(p-n)/2]}2^{-2m}\binom{p}{n+2m}\binom{n+2m}{m}. \qquad [46]$$

Note that $Q_p(n)$ does not depend on the spin I but is completely determined by the form [40] of the ESEEM. The product $\cos(n_\alpha\alpha)\cos(n_\beta\beta)$—which is named modulation pair and abbreviated as (n_α, n_β)—could also be written as $[\cos(n_\alpha\alpha + n_\beta\beta) + \cos(n_\alpha\alpha - n_\beta\beta)]/2$ to show that it is equivalent to two combination modulations (sum and difference) with halved amplitude. However, when at least one modulation index is zero, the modulation pair reduces to a single modulation with full amplitude. Therefore, it is convenient to write such modulation pairs as a product so that the additional factor $\frac{1}{2}$ is automatically accounted for. Looking at the summation limits in Eq. [45], we see that n_α and n_β range from 0 to p. The other way round, a given pair (n_α, n_β) appears in W_n^p only when $p \geqslant \tilde{n} = \max(n_\alpha, n_\beta)$. There are then $(p+1)^2$ modulation pairs among which one can recognize a zero-frequency term ($n_\alpha = n_\beta = 0$), pure α or pure β modulations ($n_\beta = 0$ or $n_\alpha = 0$, respectively), and combination modulations ($n_\alpha \neq 0$ and $n_\beta \neq 0$).

The sum of all the modulations, each weighted according to Eqs. [33] and [45], is

$$V_n(I) = \sum_{p=0}^{2I}2^{-p}C_p(I)k^p \times\sum_{n_\alpha=0}^{p}\sum_{n_\beta=0}^{p}Q_p(n_\alpha)Q_p(n_\beta)\cos(n_\alpha\alpha)\cos(n_\beta\beta). \qquad [47]$$

Exchanging the summation order and remembering that the pure and combination harmonics occur at a given p value only when $p \geqslant \tilde{n}$, the explicit formula for $V_n(I)$ can now be written as

$$V_n(I) = \sum_{n_\alpha=0}^{2I} \sum_{n_\beta=0}^{2I} P(I, n_\alpha, n_\beta; k)\cos(n_\alpha\alpha)\cos(n_\beta\beta), \quad [48]$$

where

$$P(I, n_\alpha, n_\beta; k) = \sum_{p=\tilde{n}}^{2I} C_p(I)Q_p(n_\alpha)Q_p(n_\beta)\left(\frac{k}{2}\right)^p. \quad [49]$$

The amplitude $P(I, n_\alpha, n_\beta; k)$ of each modulation pair is a polynomial of degree $2I$ in k in which the lowest exponent of k is $\tilde{n}$. Each polynomial coefficient is a product of terms which depend separately on the spin I and on the two modulation indexes. In their turn, these terms are rational numbers assembled from remarkably simple blocks: the normalizing factor $2I + 1$, integer powers of 2, and factorials. The amplitude of the (n_α, n_β) modulation pair is the same as that of (n_β, n_α) since the exchange of the modulation indexes has no effect on $P(I, n_\alpha, n_\beta; k)$. There are $(2I + 1)^2$ unique modulation pairs in $V_n(I)$, out of which one is zero frequency, $2 \times 2I$ are pure α and pure β modulations, and $4I^2$ are combination modulations. Comparing the pth power of W_n with the $(p - 1)$th power, it can be seen that the former contributes to the weight of the p^2 modulation pairs already contained in the latter and that it contains $2p + 1$ new modulation pairs. There are then $2I - \tilde{n} + 1$ contributions of order $\tilde{n}, \tilde{n} + 1, \ldots, 2I$ in k to the amplitude of each (n_α, n_β) pair.

The formula for primary ESEEM is readily obtained from Eqs. [28], [48], and [49] as

$$M_2(I; \tau) = \sum_{n_\alpha=0}^{2I} \sum_{n_\beta=0}^{2I} P(I, n_\alpha, n_\beta; k)\cos(n_\alpha\omega_\alpha\tau)\cos(n_\beta\omega_\beta\tau), \quad [50]$$

where the time dependence of M_2 is shown. A $(n_\alpha, 0)$ modulation pair translates into one single modulation $\cos(n_\alpha\omega_\alpha\tau)$ with amplitude $P(I, n_\alpha, 0; k)$, while a combination modulation pair (n_α, n_β) yields the two combination (sum and difference) modulations $\cos[(n_\alpha\omega_\alpha + n_\beta\omega_\beta)\tau]$ and $\cos[(n_\alpha\omega_\alpha - n_\beta\omega_\beta)\tau]$, each with amplitude $P(I, n_\alpha, n_\beta; k)/2$. Therefore a primary ESEEM contains at most $2I + 2I + 2 \times 4I^2 = 4I(2I + 1)$ unique modulations. The formula for the two-dimensional stimulated ESEEM is

$$M_3(I; \tau, \tau') = \frac{1}{2} \sum_{n_\alpha=0}^{2I} \sum_{n_\beta=0}^{2I} P(I, n_\alpha, n_\beta; k) \times [\cos(n_\alpha\omega_\alpha\tau')\cos(n_\beta\omega_\beta\tau) + \cos(n_\alpha\omega_\alpha\tau)\cos(n_\beta\omega_\beta\tau')]. \quad [51]$$

In this case, a pure modulation pair, say $(n_\alpha, 0)$, gives rise to a modulation along each time axis [$\cos(n_\alpha\omega_\alpha\tau)$ and $\cos(n_\alpha\omega_\alpha\tau')$] with amplitude $P(I, n_\alpha, 0; k)/2$ (axial peaks). A combination modulation pair produces four modulations [$\cos(n_\alpha\omega_\alpha\tau' + n_\beta\omega_\beta\tau)$ and $\cos(n_\alpha\omega_\alpha\tau' - n_\beta\omega_\beta\tau)$ plus those with τ and τ' exchanged] with amplitude $P(I, n_\alpha, n_\beta; k)/4$ (cross peaks). Since Eq. [51] is symmetric under exchange of τ and τ', the peaks in the 2-D FT spectrum form reflecto-symmetrical pairs (*30*) about the main diagonal.

Stimulated ESEEM is most often performed as a one-dimensional experiment by holding τ fixed while varying τ', and the preceding equation can be specialized accordingly. This is not a mere exercise but it reveals features proper to the 1-D experiment. Equation [51] could be rewritten by splitting the double sum and collecting the terms independent of τ', but it takes less algebra to go back to Eq. [40] and write it for $W_{3\alpha}$ as

$$W_{3\alpha} = \tfrac{1}{2}(1 - \cos\omega_\alpha\tau')(1 - \cos\omega_\beta\tau). \quad [52]$$

The τ-dependent term is left unchanged while the other term is manipulated exactly as in the general case. One arrives quickly at

$$V_{3\alpha}(I) = 2\sum_{n=0}^{2I} S(I, n; \omega_\beta\tau, k)\cos(n\omega_\alpha\tau'), \quad [53]$$

where

$$S(I, n; \omega_\beta\tau, k) = \frac{1}{2}\sum_{p=n}^{2I} C_p(I)Q_p(n)(1 - \cos\omega_\beta\tau)^p\left(\frac{k}{2}\right)^p. \quad [54]$$

As before, $V_{3\beta}(I)$ is obtained from $V_{3\alpha}(I)$ by exchanging α and β everywhere. The product $(1 - \cos\omega_\beta\tau)k$ can be considered as an effective τ-dependent modulation depth parameter, which ranges from 0 to $2k$. Note that, for a given τ, the effective modulation depth parameter for the ω_β modulations has a different value. The 1-D stimulated ESEEM can then be written as

$$M_3(I; \tau') = \sum_{n=0}^{2I} S(I, n; \omega_\beta\tau, k)\cos(n\omega_\alpha\tau') + S(I, n; \omega_\alpha\tau, k)\cos(n\omega_\beta\tau'). \quad [55]$$

Comparing this with the 2-D stimulated ESEEM formula, it can be seen that there are no combination modulations since the double summation has been converted to a single summation which runs over only one modulation index. The number of modulations is thus reduced to $4I$, neglecting the zero-frequency terms. The suppression effect, well known for $I = \frac{1}{2}$, exists also for arbitrary I since the amplitude of the ω_μ modulation depends on $1 - \cos \omega_\nu \tau$ ($\mu \neq \nu$). In general, different $n\omega_\mu$ harmonics are affected to a different extent by the suppression effect except when $1 - \cos \omega_\nu \tau = 0$, since then all $n\omega_\mu$ harmonics vanish (blind spot).

The Fourier transformation of Eqs. [50], [51], and [55] would give the analytical form of the frequency-domain ESEEM spectra. However, the position and the amplitude of each frequency-domain peak can be obtained by inspection of these equations, bearing in mind that the amplitude of the combination harmonics is equally divided between the sum and difference peaks. The general Eqs. [27], [33], and [48] are the central result of this paper. From them, I derived the ESEEM formulas for primary and stimulated ESEEM for arbitrary I which are based on the same approximations and have the same validity as the well-known Eqs. [30] and [31] for $I = \frac{1}{2}$.

ANALYSIS OF THE SPECTRAL AMPLITUDES

In the previous section, it was shown that the modulation amplitude in primary and stimulated ESEEM experiments is given by the polynomials $P(I, n_\alpha, n_\beta; k)$ and $S(I, n; \omega_\mu \tau, k)$ of degree $2I$ in k. In this section, we analyze in some detail the importance of the nonlinear terms with respect to the linear term and the amplitude of the modulations as a function of the modulation depth parameter. The vast majority of natural stable nuclides bear half-integer spin (32) ranging from $\frac{1}{2}$ to $\frac{9}{2}$, the most notable exceptions being ^{2}H and ^{14}N which have spin 1; stable nuclides with integer spin $I \neq 1$ (^{6}Li, ^{10}B, and ^{50}V) are rarely observed in EPR spectroscopy. In the following discussion, I therefore consider only the $I = 1$ case in addition to the half-integral values $I = \frac{1}{2}, \frac{3}{2}, \frac{5}{2}, \frac{7}{2}, \frac{9}{2}$.

The amplitude of the modulations in primary and 2-D stimulated ESEEM is given in Eq. [49]. The occurrence of higher harmonic modulations is entirely due to the nonlinearity of the ESEEM with respect to k. Indeed, the linear term contributes only to the amplitude of the fundamental modulations ($\tilde{n} = 1$), and since $0 \leqslant k \leqslant 1$, one might think that the high-order terms are always less significant than the linear term. This is not true since the polynomial coefficients can be very large, as illustrated in Fig. 2 which shows the absolute value of the ratio

$$R_p(I, 1, 0; k) = \frac{C_p(I) Q_p(1) Q_p(0)}{C_1(I) Q_1(1) Q_1(0)} \left(\frac{k}{2}\right)^{p-1} \qquad [56]$$

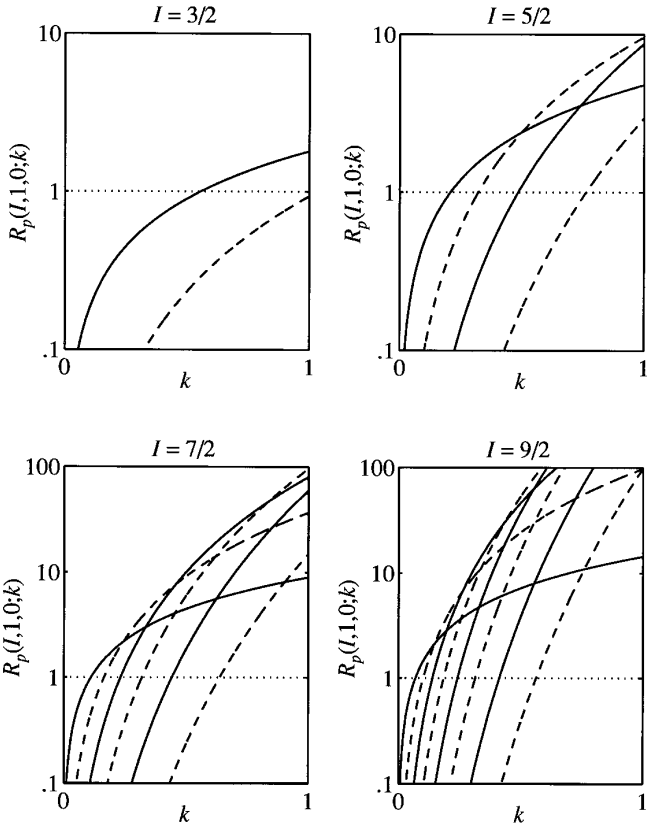

FIG. 2. Absolute value of the ratio $R_p(I,1,0; k)$ of the term of order p in k to the linear term ($p = 1$) contributing to the amplitude of the fundamental pure harmonic (1, 0) in primary and 2-D stimulated ESEEM. Positive $R_p(I,1,0; k)$ are represented by a solid line, negative by dashed lines. The curve that crosses the horizontal axis closest to the origin represents $p = 2$, the second closest represents $p = 3$, and so on.

of the pth-order term to the linear term contributing to the amplitude of the fundamental (1, 0) modulation for selected I values. At $k \cong 0$, the linear term is of course dominant but the nonlinear terms soon become significant. The quadratic ($p = 2$) term can even overtake the linear term when $I \geqslant \frac{3}{2}$, and it shows up at smaller k on increasing I. Also the $p > 2$ terms can be larger than the linear term when $I \geqslant \frac{5}{2}$, and as before, the high-order terms grow faster for larger I since $R_p(I, 1, 0; k)$ is proportional to $I^{2(p-1)}$. When k approaches 1, the linear term is often the least contribution to the modulation. It should also be noted that terms of different order alternate in sign as can be seen in Fig. 2 where, for any I, $R_p(I, 1, 0; k)$ is positive for odd p and vice versa. This holds also for any other modulation, as the sign of $Q_p(n_\alpha) Q_p(n_\beta)$ is determined by the modulation indexes, whereas that of $C_p(I)$ is fixed by the parity of p. Therefore, the modulation amplitudes are not increasing throughout the $0 \leqslant k \leqslant 1$ interval but they are oscillating functions with maxima and minima.

The amplitude of the ESEEM arising from a high-spin

TABLE 2

Modulation-Depth Parameter k for Which the Amplitude Error Arising from the Neglect of Nonlinear Terms Is 10 and 50% of the True Amplitude for the Indicated Modulations

	(1, 0)		(1, ±1)	
I	10% error	50% error	10% error	50% error
1	0.122	0.445	0.097	0.334
$\frac{3}{2}$	0.052	0.208	0.039	0.153
$\frac{5}{2}$	0.020	0.082	0.015	0.060
$\frac{7}{2}$	0.011	0.045	0.008	0.033
$\frac{9}{2}$	0.007	0.028	0.005	0.021

nucleus can then be a largely nonlinear function of the modulation depth parameter, and the value of k at which nonlinearity becomes significant becomes smaller as I increases, as can be appreciated from Table 2, where the values of k, at which the amplitude error arising from the neglect of nonlinear terms is 10 and 50% of the true amplitude for the fundamental modulations, are reported. It is interesting at this point to compare the above results with those from an earlier analysis (*5*) of the primary ESEEM due to a nucleus of arbitrary spin which neglected the nuclear quadrupole interaction and the terms of second and higher order in k in the modulation amplitude. From such approximate analysis, it was found that the primary ESEEM due to a nucleus of arbitrary spin is given by Eq. [30] provided that $\frac{4}{3}I(I+1)k$ is substituted for k. This result can be reproduced and extended to stimulated ESEEM by retaining only the first-order terms in the amplitudes, which are then zero except for the fundamental modulation. Thus, Eq. [48] becomes

$$V_n(I) = 1 - \frac{k}{2} C_1(I)(1 - \cos\alpha - \cos\beta + \cos\alpha\cos\beta) = 1 - \frac{4}{3} I(I+1)k\left[\frac{1}{2}(1 - \cos\alpha)(1 - \cos\beta)\right] \quad [57]$$

as expected. However, this expression is valid only when nonlinearity is negligible, that is, for small k values, since the terms of second and higher order in k become quickly significant, as shown in Fig. 2 and in Table 2. From the latter, it can be seen that the linearized expression does not lead to severe errors for $I = 1$ nuclei, such as deuterium, as long as k is smaller than about 0.1, but it is not tenable for large-I nuclei: for $I = \frac{9}{2}$, a 50% error is introduced for k as small as 0.03. Of course, the linearized expression does not contain any modulation harmonics and incorrectly suggests that large modulations can be obtained only with large k (*vide infra*).

I consider now the spectral amplitudes of the modulations as a function of the modulation depth parameter k. The amplitudes $P(I, n, 0; k)$ of the pure harmonics $(n, 0)$ are plotted in Fig. 3. Recall that the $(0, n)$ modulations have the same amplitude as the $(n, 0)$ modulations. For any value of k, the amplitudes are positive and the deepest modulation is always $(1, 0)$, the second deepest $(2, 0)$, and so on. No modulation has amplitude greater than 0.5, a limiting value attained only in the case of a $I = \frac{1}{2}$ nucleus with $k = 1$. At very small k values, the amplitude behaves as the nth power of k since there $P(I, n, 0; k) \cong C_n(I)Q_n(n)Q_n(0)(k/2)^n$. Then the fundamental modulation $(1, 0)$ dominates over the its harmonics and the ESEEM spectrum is rather simple. The initial slope of the pure modulation amplitudes grows rapidly with I: considering the expression of $C_n(I)$, one finds that the initial slope of the $(n, 0)$ modulation is proportional to I^{2n}, e.g., it is $\frac{2}{3}I(I+1)$ for $n = 1$. Then ESEEM spectroscopy is extremely sensitive to high-spin nuclei when k is small.

Another striking difference in the behavior of the pure-

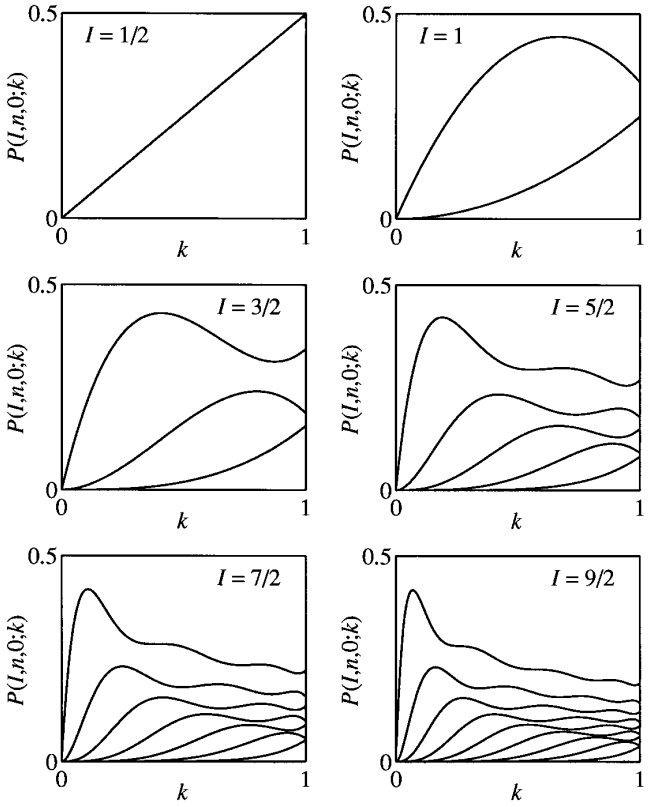

FIG. 3. Amplitude $P(I, n, 0; k)$ of the pure modulations $(n, 0)$ in primary ESEEM against the modulation depth parameter k. The largest amplitude corresponds to $(1, 0)$, the second largest to $(2, 0)$ and so on. The amplitude of the pure harmonics in 2-D stimulated ESEEM is $P(I, n, 0; k)/2$.

TABLE 3
Modulation-Depth Parameter k for Which the Absolute Value of the Amplitude of the Indicated Modulations Is Maximum

I	(1, 0)	(2, 0)	(1, ±1)	(1, ±2)
$\frac{1}{2}$	1.000		1.000	
1	0.667	1.000	0.500	1.000
$\frac{3}{2}$	0.408	0.800	0.275	0.711
$\frac{5}{2}$	0.190	0.421	0.119	0.335
$\frac{7}{2}$	0.108	0.249	0.067	0.190
$\frac{9}{2}$	0.070	0.163	0.042	0.122

modulation amplitudes between the $I > \frac{1}{2}$ case and the usual $I = \frac{1}{2}$ case is recognized when one considers moderate to large values of k. In fact, only the highest harmonic $(2I, 0)$ increases monotonically as for $I = \frac{1}{2}$; the other pure modulations reach a maximum amplitude and then slowly decay while oscillating. The number of crests and troughs decreases in the higher harmonics and the highest one $(2I, 0)$ has none, as already noted. For a given I, the maximum-amplitude k value becomes larger for higher harmonics, whereas for a given n, it becomes smaller at larger I values. The value at which $P(I, 1, 0; k)$ is maximum ranges from $k = 1$ $(I = \frac{1}{2})$ to a much smaller $k = 0.07$ $(I = \frac{9}{2})$, as shown in Table 3. At large k, the $n > 1$ harmonics may make the ESEEM spectrum much more complicated.

As discussed in the preceding section, the combination pair (n_α, n_β) represents the two distinct sum and difference modulations. In the following, the phrase ''spectral amplitude'' means the amplitude $P(I, n_\alpha, n_\beta; k)/2$ of whichever of the two modulations is associated with the pair (n_α, n_β). In Fig. 4a are plotted the spectral amplitudes of the symmetric combination modulations $\omega_\alpha \pm \omega_\beta$ and of the asymmetric ones $\omega_\alpha \pm 2\omega_\beta$ for several I values. Like the pure modulations, the combination modulations have zero spectral amplitude at $k = 0$, reach an extreme value, and then decay. The behavior of the initial slope and of the position of maximum spectral amplitude as a function of I is similar to that of the pure modulations: the value at which $P(I, 1, 1; k)$ is maximum ranges from $k = 1$ $(I = \frac{1}{2})$ to a much smaller $k = 0.042$ $(I = \frac{9}{2})$, as shown in Table 3. The spectral amplitudes $P(\frac{7}{2}, n_\alpha, n_\beta, k)/2$ of the most important combination modulations arising from a $I = \frac{7}{2}$ nucleus are plotted in Fig. 4b. The initial slope can be either positive or negative, and its absolute value decreases for higher harmonics. Considering the lowest order coefficient $C_{\tilde{n}}(I)Q_{\tilde{n}}(n_\alpha)Q_{\tilde{n}}(n_\beta)$, one finds that the initial slope is positive (negative) when $\min(n_\alpha, n_\beta)$ is even (odd). It is apparent that the higher harmonics are generally weaker but tend to be more important for large k values. There the spectrum becomes very complicated since several combination lines have comparable amplitude. It should also be noted that, at variance with pure modulations, the amplitudes of the combination modulations do cross each other so that the larger one is not always that with the lowest index. However, the most striking feature in Fig. 4 is that the spectral amplitude of the combination harmonics can change sign, so that the phase of a combination line may be different for different samples or for the same sample at different magnetic fields or even within the powder-like envelope of the combination peaks from a disordered sample. Of course, this also means that the spectral amplitude of a combination line may drop to zero for certain k values. This is a new type of suppression effect, which can occur only for combination modulations and for $I > \frac{1}{2}$. It arises from the interference of electron coherence-transfer echoes (*24*) which are modulated at the same frequency but stem from transfer of electron coherence between different level pairs. Its physical origin is then different from that of the suppression effect in 1-D stimulated ESEEM of $I = \frac{1}{2}$ nuclei which arises from the τ-dependent amplitude of the nuclear coher-

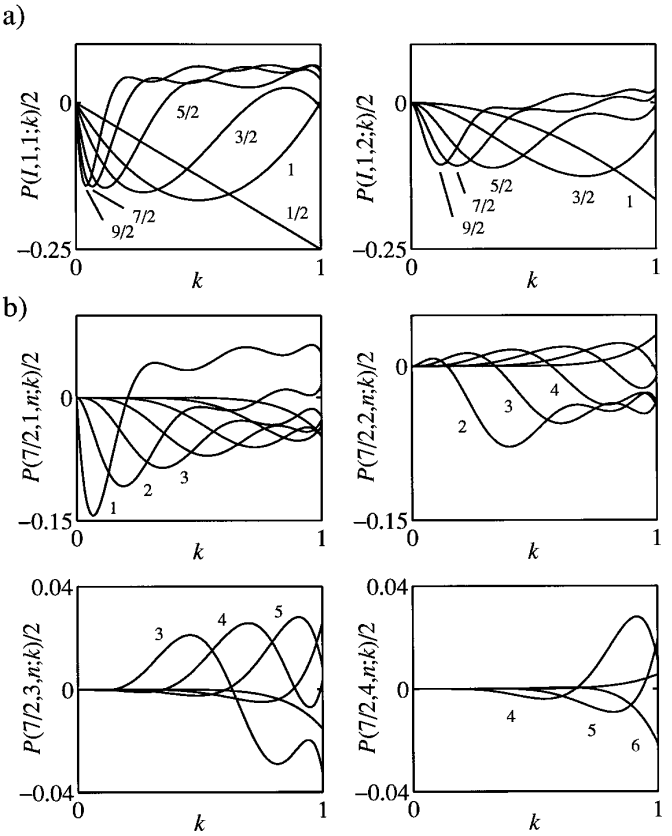

FIG. 4. (a) Amplitude $P(I, 1, 1; k)/2$ and $P(I, 1, 2; k)/2$ of the combination modulations in primary ESEEM. The curves are labeled by the nuclear spin quantum number I. The amplitude of the corresponding harmonics in 2-D stimulated ESEEM is halved. (b) Amplitude $P(7/2, n_\alpha, n_\beta; k)/2$ of the most significant combination harmonics in the primary ESEEM for a nucleus with spin $\frac{7}{2}$. In each panel are collected the modulations with fixed n_α and n_β ranging from n_α to $2I + 1 = 7$. Some curves are labeled by the β modulation index n_β; the other labels can be easily inferred.

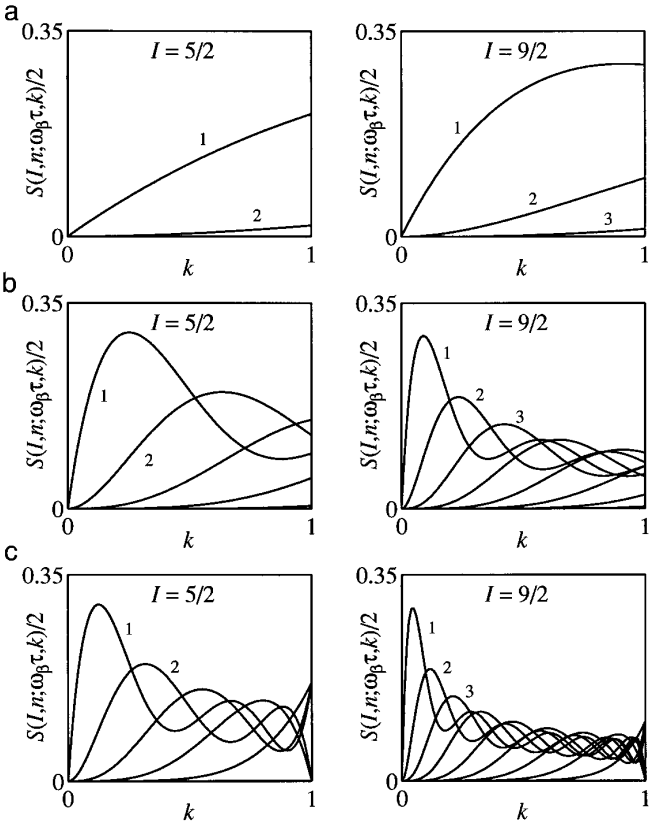

FIG. 5. Amplitude $S(I, n; \omega_\beta\tau, k)$ of the modulations arising from a nucleus with spin $I = \frac{5}{2}$ or $I = \frac{9}{2}$ in 1-D stimulated ESEEM. The modulation index n is reported only for the first few harmonics, the others can be easily inferred. The value of the suppression factor $1 - \cos \omega_\beta\tau$ is: (a) 0.1, (b) 1.0, (c) 2.0.

ences excited by the $\pi/2 — \tau — \pi/2$ subsequence. Being independent of any time interval of the pulse sequence, the new suppression effect can be coped with only by performing the experiment at another microwave frequency where the nuclear Zeeman interaction and thus the modulation depth parameter are different.

The 1-D stimulated ESEEM features only the pure modulations $(n, 0)$ and $(0, n)$, the amplitudes of which are given in Eq. [54]. As in primary and 2-D stimulated ESEEM, the modulation amplitudes may be a largely nonlinear function of the modulation-depth parameter. The analysis of the relative importance of the different terms in $S(I, n; \omega_\mu\tau, k)$ is similar to that of the previously discussed experiments and it is not worthwhile repeating. If suffices to say that the 1-D stimulated ESEEM amplitudes are in general slightly less sensitive to high-order terms. Without loosing generality, I consider in the following only the $(n, 0)$ modulations. In Fig. 5 are plotted the amplitudes $S(I, n; \omega_\beta\tau, k)$ of the modulations $(n, 0)$ arising from a nucleus of spin $I = \frac{5}{2}$ or $\frac{9}{2}$ for different values of $\omega_\beta\tau$. The behavior of the modulation amplitudes is similar to that of the pure modulations in primary ESEEM: all amplitudes are positive for any values of the suppression factor $(1 - \cos \omega_\mu\tau)$ and of the modulation depth parameter k. In the vicinity of a blind spot, $\cos(\omega_\beta\tau) \cong 1$ so that the lowest-order term in $S(I, n; \omega_\beta\tau, k)$ becomes largely dominant (Fig. 5a, $1 - \cos \omega_\beta\tau = 0.1$). Then the amplitude of $(n, 0)$ is proportional to k^n and the fundamental harmonic $(1, 0)$ is much larger than any other $(n > 1, 0)$ modulation. In other words, on approaching a blind spot, the higher is the harmonic, the quicker it vanishes. The product $(1 - \cos \omega_\mu\tau)k$ could be considered as an effective τ-dependent modulation depth parameter which can be varied between 0 and $2k$. The experimenter can then trade sensitivity for simplification of the ESEEM spectrum by choosing a τ value close to a blind spot.

When $1 - \cos \omega_\beta\tau = 1$ (Fig. 5b), the amplitude of the ω_α modulations is free from suppression effects, therefore 1-D stimulated ESEEM is best compared with primary ESEEM. Comparing Fig. 5 with Fig. 3, one immediately notices that in 1-D stimulated ESEEM the harmonics are more important with respect to the fundamental, and the number of extremes in correspondent modulations is largely reduced. The most important difference is however that the amplitudes of the harmonics in 1-D stimulated ESEEM cross each other (this occurs only when $I \geqslant \frac{5}{2}$). As for the combination modulations, one cannot pick out the fundamental modulation by inspection of the spectrum since it is not always the largest one. When k is large, the modulations have similar amplitude and the spectrum becomes more crowded. This trend is even more evident when τ is such that $1 - \cos \omega_\beta\tau = 2$ (Fig. 5c): all the harmonics have about the same amplitude. Note also that at $k = 1$ the even harmonics vanish,[1] whereas the odd harmonics have amplitude $\frac{1}{6}$ for $I = \frac{5}{2}$ and $\frac{1}{10}$ for $I = \frac{9}{2}$.

SPECTRAL SIMULATIONS

Without knowledge of the analytical formulas, the ESEEM arising from a nucleus of arbitrary spin can be computed by numerical simulation of the time evolution of the spin system during the experiment, e.g., using the GAMMA (*33*) routine library, but such calculations require a considerable amount of computing time. The previously developed theory provides two much faster methods for the numerical simulation of the ESEEM. The analytical formulas can be implemented in a computer program, thus saving a large fraction of computing time. However, this procedure still

[1] This is a special case of a more general rule valid for 1-D stimulated ESEEM. When $(1 - \cos \omega_\beta\tau)k = 2$ and I is half-integer (integer), the even (odd) ω_α harmonics vanish, whereas the odd (even) harmonics have amplitude $1/(2I + 1)$. This rule can be easily proved by noting that in this case $V_{3\alpha}(\frac{1}{2}) = \cos \omega_\alpha\tau'$ and $V_{3\alpha}(I) = [1/(2I + 1)]\sin[(2I + 1)\omega_\alpha\tau']/\sin \omega_\alpha\tau'$. Simplifying the fraction and recalling that $M_3(I; \tau') = [V_{3\alpha}(I) + V_{3\beta}(I)]/2$, one demonstrates the general rule.

TABLE 4
Comparison of the Time Needed to Compute a Primary ESEEM Trace for a System Consisting of One Electron and One Nucleus with Spin I by Different Procedures

	Relative computing time		
	$I = \frac{1}{2}$	$I = \frac{5}{2}$	$I = \frac{9}{2}$
Time evolution of the spin system	85	390	1390
Analytical formula	1	4	16
Analytical formula for $I = \frac{1}{2}$ plus tranformation by the Chebyshev polynomials (C++ program)	1	2	3
Analytical formula for $I = \frac{1}{2}$ plus transformation by the Chebyshev polynomials (Matlab program)	1	1	1

involves a large number of evaluations of polynomials and cosine functions which can be substantially reduced using a computing strategy in two steps: (1) the ESEEM is calculated for nuclear spin $I = \frac{1}{2}$, the other conditions being the same; (2) the $V_n(\frac{1}{2})$ are transformed into the $V_n(I)$ following Eq. [27] to get the desired ESEEM. The last method requires only the knowledge of the analytical formula for $I = \frac{1}{2}$ and of its partition into the $V_n(I)$ so that it can be used to simulate experiments also when the corresponding formula for arbitrary spin would be exceedingly complicated, e.g., experiments based on the four-pulse sequence ($\pi/2$—τ—$\pi/2$—t_1—π—t_2—$\pi/2$—τ) such as HYSCORE (*34*), DEFENCE (*35*), CF (*36*), HF (*37*), and several others (*37, 38*). All three procedures have been implemented as C++ programs compiled with the GNU C++ compiler (version 2.5.8) and the GAMMA library (version 3.3), and have been run on an IBM RISC System/6000 Model 355H workstation. They produced identical spectra for a wide range of spin systems. The relative speed of the three programs is reported in Table 4 for the simulation of a primary ESEEM trace with $I = \frac{1}{2}, \frac{5}{2}$, and $\frac{9}{2}$. The availability of the analytical formula enables a large reduction in computing time, about two orders of magnitude. A further substantial reduction can be obtained by the procedure based on the calculation of the $V_n(\frac{1}{2})$. The computing time can be even further reduced, especially for large I, by implementing the latter procedure in an environment optimized for numerical calculations, such as Matlab (*39*). All the simulations presented in this section were carried out using this last method. The computer programs in C++ and Matlab languages are available from the author upon request.

Simulations of primary and 1-D stimulated ESEEM are now presented in order to illustrate the characteristics proper to nuclei with $I > \frac{1}{2}$ which were remarked in the previous section. A single orientation of the external magnetic field with respect to the hyperfine principal axes is taken into account in these simulations, which are then examples of the ESEEM observed in ordered systems such as single crystals. Since the goal of the present section is to show how the peculiar dependence of the modulation amplitude on the modulation depth parameter affects the spectral shape, the ESEEM simulations are reported as properly phased cosine-FT spectra. Such spectra can be obtained from real experiments when the ''deadtime'' problem is coped with either by mathematical (*40*) or by instrumental techniques, such as pulse-swapping (*29*), remote-echo detection (*41*), and echo-modulation echo (*42*).

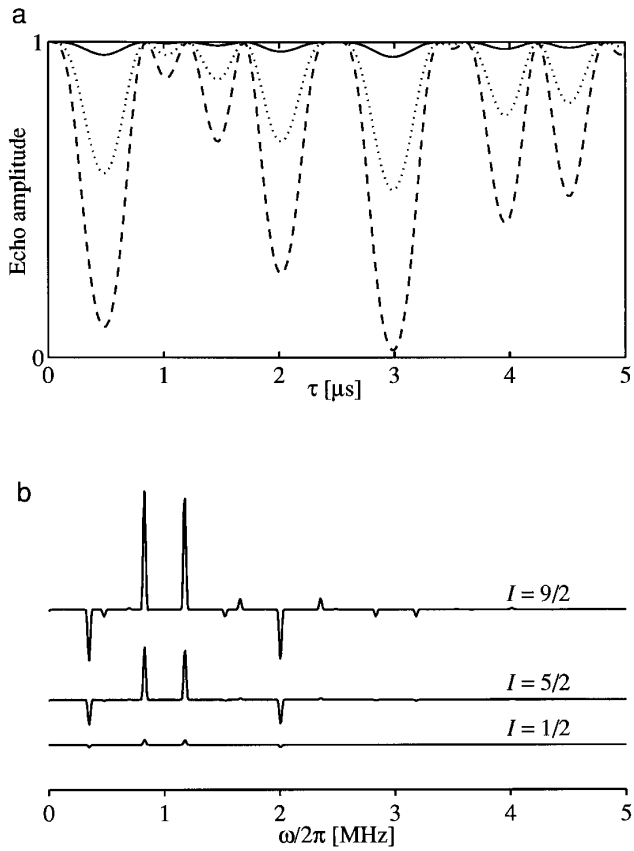

FIG. 6. Primary ESEEM of an ordered $S = \frac{1}{2}$, $I = (\frac{1}{2}, \frac{5}{2}, \frac{9}{2})$ system. Simulation parameters: $\omega_I/2\pi = 1.0$ MHz, $A_\parallel/2\pi = 0.5$ MHz, $A_\perp/2\pi = 0.2$ MHz, $\theta = 45°$. (a) Time-domain traces; solid line, $I = \frac{1}{2}$; dotted line, $I = \frac{5}{2}$, dashed line, $I = \frac{9}{2}$. (b) Spectra obtained by cosine FT of the trace after baseline correction, apodization with a Kaiser window, and zero filling.

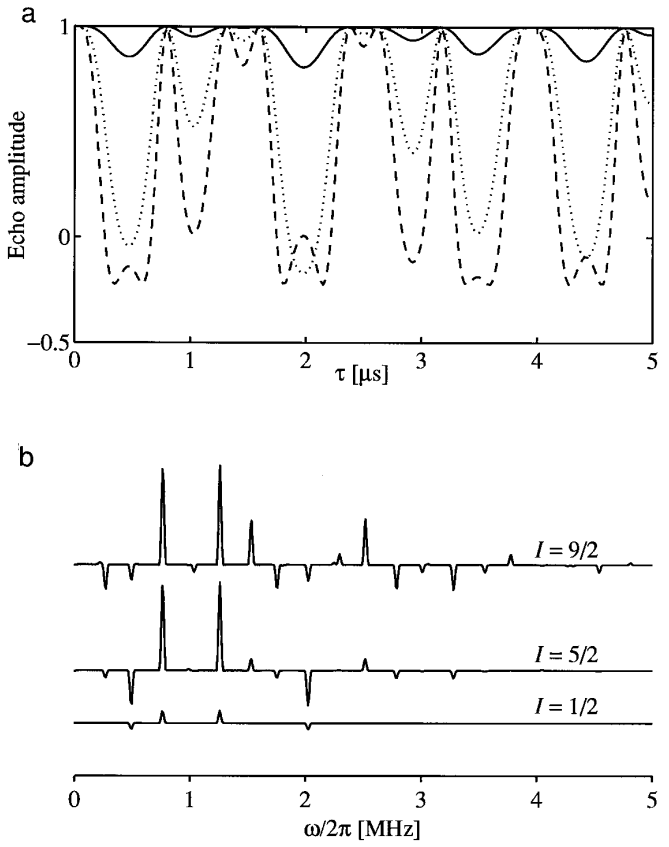

FIG. 7. Primary ESEEM of an ordered $S = \frac{1}{2}$, $I = (\frac{1}{2}, \frac{5}{2}, \frac{9}{2})$ system. Simulation parameters: $\omega_I/2\pi = 1.0$ MHz, $A_\parallel/2\pi = 0.8$ MHz, $A_\perp/2\pi = 0.2$ MHz, $\theta = 45°$. (a) Time-domain traces; solid line, $I = \frac{1}{2}$; dotted line, $I = \frac{5}{2}$; dashed line, $I = \frac{9}{2}$. (b) Spectra obtained by cosine FT of the trace after baseline correction, apodization with a Kaiser window, and zero filling.

The greater sensitivity to high-spin nuclei even at small k values is illustrated in Fig. 6 where the primary ESEEM traces and the correspondent FT spectra for three systems consisting of one electron and one nucleus with spin $I = \frac{1}{2}$, $\frac{5}{2}$, and $\frac{9}{2}$ are reported. The nuclei are subject to an axial hyperfine interaction ($A_\parallel/2\pi = 0.5$ MHz, $A_\perp/2\pi = 0.2$ MHz, $\omega_I/2\pi = 1.0$ MHz); the angle θ between $\mathbf{B}_0$ and the unique axis of the hyperfine interaction is 45°. The modulation depth parameter at this orientation is $k = 0.024$ and then the $I = \frac{1}{2}$ ESEEM amounts only to a few percent of the echo amplitude, whereas the $I = \frac{5}{2}$ ESEEM is very deep, attaining about 50% of the echo amplitude, and that for $I = \frac{9}{2}$ is about twice as deep. Such very large enhancement of the modulation depth can be traced back to the large modulation amplitudes at small k for high-spin nuclei as pictured in Figs. 3 and 4a. Since k is small, the $n > 1$ modulations are rather weak, but the amplitude of the fundamental modulations is already significantly affected by high-order terms (cf. Table 2). Nonlinearity shows up as soon as k becomes a little larger. Figure 7 shows the primary ESEEM traces and the correspondent FT spectra for the three spin systems considered subject to a slightly larger hyperfine interaction ($A_\parallel/2\pi = 0.8$ MHz, $A_\perp/2\pi = 0.2$ MHz, $\omega_I/2\pi = 1.0$ MHz, $\theta = 45°$). The modulation depth parameter at this orientation is $k = 0.097$. The different shapes of the time traces and the presence of many harmonics in the cosine-FT spectra is already evidence of the nonlinearity but it is perhaps more striking that the ω_α and ω_β peaks ($\omega/2\pi = 1.27$ and 0.79 MHz, respectively) have similar amplitude for $I = \frac{5}{2}$ and $I = \frac{9}{2}$ (cf. Fig. 3) and that the $\omega_\alpha \pm \omega_\beta$ combination peaks at $\omega/2\pi = 2.06$ and 0.48 MHz are smaller for $I = \frac{9}{2}$ than they are for $I = \frac{5}{2}$ (cf. Fig. 4a).

The high-order modulations are even more prominent when k is large as pictured in Fig. 8a where the cos-FT primary ESEEM spectrum for a nucleus with spin $\frac{9}{2}$ and hyperfine coupling falling in the matched (*43*) range ($A_\parallel/2\pi = 2.7$ MHz, $A_\perp/2\pi = 1.8$ MHz, $\omega_I/2\pi = 1.0$ MHz, $\theta = 45°$) is reported. Since $k = 0.669$, the ESEEM is extremely nonlinear and the spectrum is very crowded and difficult to interpret if even a single nucleus is present. The amplitude of the pure modulations decreases steadily when the modulation index gets larger. On the contrary, that of the combination modulations does not follow any simple rule as shown

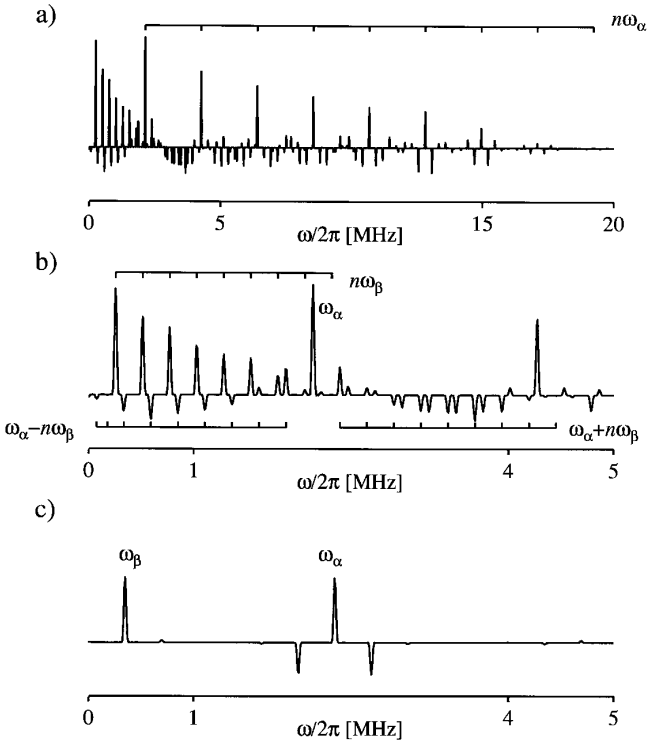

FIG. 8. Cosine-FT primary ESEEM spectra of an ordered $S = \frac{1}{2}$, $I = \frac{9}{2}$ system with hyperfine coupling in the matched range. Simulation parameters: $\omega_I/2\pi = 1.0$ MHz, $A_\parallel/2\pi = 2.7$ MHz, $A_\perp/2\pi = 1.8$ MHz. (a) $\theta = 45°$, (b) enlargement of (a), (c) $\theta = 5°$. The time-domain traces were baseline corrected, apodized with a Kaiser window, and zero filled prior to FT.

by the $\omega_\alpha \pm n\omega_\beta$ modulations, best visible in the enlargement (Fig. 8b). Such behavior can be understood by comparing the spectra with Fig. 4. Indeed, it is noteworthy that the fundamental combination modulations at frequency $(\omega_\alpha + \omega_\beta)/2\pi = 2.39$ MHz and $(\omega_\alpha - \omega_\beta)/2\pi = 1.88$ MHz are positive and about as large as the $\omega_\alpha \pm 6\omega_\beta$ modulations.

We have just seen that when $I > \frac{1}{2}$, a small k value can be better than a large one with regard both to *sensitivity* and to *resolution* since the fundamental modulations are large and dominant. Another advantage stems from the fact that the modulation depth parameter is small near the principal directions of the hyperfine interaction. Therefore, a complicated single-crystal spectrum may be simplified by rotating the sample until one of the hyperfine principal directions is nearly aligned with the external field. This property also paves the way for directly measuring the principal values of the hyperfine interaction by means of ESEEM spectroscopy: in fact, the peak amplitude still vanishes exactly at the principal directions, but it is quite large in proximity to them. This is illustrated in Fig. 8c which shows the cos-FT primary ESEEM spectrum for the same system as before but at a different orientation ($\theta = 5°$, $k = 0.009$). The fundamental modulations largely dominate the spectrum and $A_\parallel/2\pi$ can be measured from $(\omega_\alpha - \omega_\beta)/2\pi = 2.696$ MHz with great accuracy. Of course, the correspondence of small k with large amplitude can be beneficial also to disordered-system spectra which would show intense features very near to the hyperfine principal directions.

When the primary ESEEM spectrum is too crowded, it is advisable to perform 1-D stimulated ESEEM experiments to get rid of all the combination harmonics. The price one must pay is, of course, the occurrence of the suppression effect. The cos-FT 1-D stimulated ESEEM spectra for a nucleus with spin $\frac{9}{2}$ with the same parameters as before ($k = 0.669$ at $\theta = 45°$) are reported in Fig. 9. The top spectrum is computed for $\tau = 835$ ns where the suppression factors are $(1 - \cos \omega_\alpha\tau) \cong (1 - \cos \omega_\beta\tau) \cong 0.78$. It is much less crowded than the corresponding primary spectrum even if many harmonics are significant. Note the oscillations in the modulation amplitudes already remarked on in the discussion of Fig. 5. The suppression effect can be used to simplify the spectrum. By choosing τ in the vicinity of a blind spot, the high-order modulations are preferentially suppressed as illustrated by the spectra in the middle and at the bottom of the Fig. 9 which are computed with $\tau = 902$ ns $(1 - \cos \omega_\alpha\tau = 0.10)$ and $\tau = 279$ ns $(1 - \cos \omega_\beta\tau = 0.10)$, respectively. In this case, the fundamental modulations can be easily picked out not only because the higher harmonics are extensively suppressed but also because they have a larger amplitude when the effective modulation depth is small.

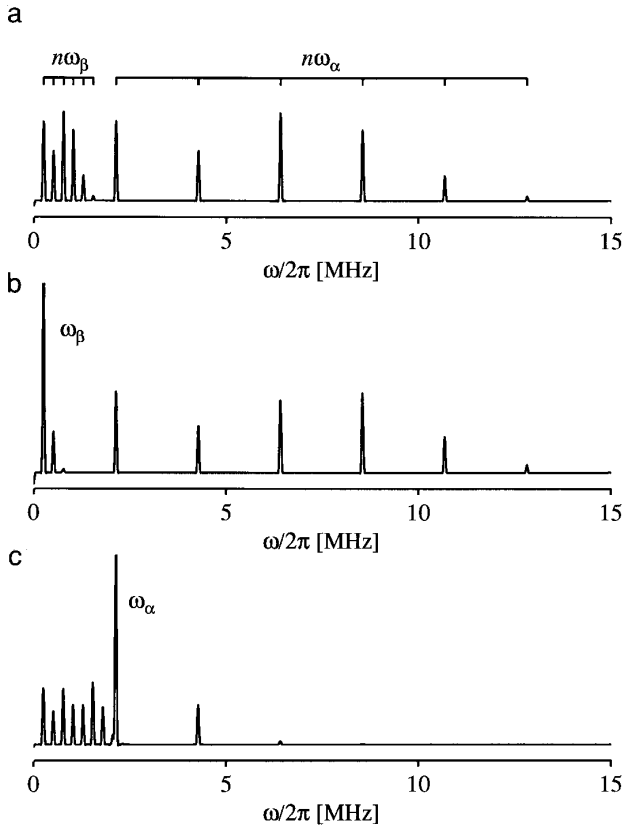

FIG. 9. Cosine-FT 1-D stimulated ESEEM spectra for an ordered $S = \frac{1}{2}$, $I = \frac{9}{2}$ system with hyperfine coupling in the matched range. Simulation parameters: $\omega_I/2\pi = 1.0$ MHz, $A_\parallel/2\pi = 2.7$ MHz, $A_\perp/2\pi = 1.8$ MHz, $\theta = 45°$. The time-domain traces were baseline corrected, apodized with a Kaiser window, and zero filled prior to FT. (a) $\tau = 835$ ns, (b) $\tau = 902$ ns, (c) $\tau = 279$ ns.

CONCLUSIONS

The electron-spin-echo envelope modulation arising from the hyperfine coupling to a nucleus of arbitrary spin I has been considered in this paper. First, it has been shown that the ESEEM resulting from any pulse sequence made up of nonselective microwave pulses and free-evolution periods can be expressed as the trace of a rotation matrix acting in the $(2I + 1)$-dimensional Hilbert subspace associated with the nuclear spin, provided that the high-field approximation is valid. Then, by resorting to the group-theoretical description of rotations, the ESEEM due to a spin $I > \frac{1}{2}$ has been expressed as a Chebyshev polynomial of the second kind where the independent variable is the ESEEM for a hypothetical $I = \frac{1}{2}$ nucleus subject to the same interactions as the real one. The ESEEM of $I > \frac{1}{2}$ nuclei then contain several harmonics of the modulation frequencies observed in the $I = \frac{1}{2}$ case and the modulation amplitudes are polynomials of degree $2I$ in the modulation depth parameter k. The general theory has been applied to the primary and to the 1-D and 2-D stimulated ESEEM experiments for which explicit analytical formulas for coupling to a nucleus of arbitrary spin have been obtained as linear combinations of cosine functions; the arguments thereof contain the modulation frequencies.

The central result of the theory developed is that the modulation amplitudes depend on k in a largely *nonlinear* way. This introduces two differences with respect to the ESEEM of spin-$\frac{1}{2}$ nuclei. First, the amplitudes of the fundamental pure and combination modulations, already present in the $I = \frac{1}{2}$ case, are nonlinear functions of k; second, harmonics of the fundamental modulations (up to the $2I$th one) appear in the ESEEM with amplitudes which can be comparable with those of the fundamental modulations. As a general rule, nonlinear effects are more important when I is large, provided that all the other factors are the same. In all the three ESEEM experiments considered, the modulation amplitudes show a similar behavior. When k is very small, they are proportional to $k^{\tilde{n}}$; when k becomes larger, they reach a maximum (in absolute value) and then slowly decay with oscillations since terms of different order alternate in sign. The shape of these curves depend strongly on the nuclear spin: when I is larger, the initial slope is steeper, the maximum amplitude is reached at smaller k, and there are more oscillations.

While the amplitude of the pure modulation is always positive, the sign of the combination ones in primary (and 2-D stimulated) ESEEM depends on k, and then their amplitude vanishes for one or more k values irrespective of τ. This new suppression effect arises from the interference of electron coherence-transfer echoes which modulate the echo at the same frequency but stem from transfer of electron coherence between different level pairs. Its physical origin is then different from that of the suppression effect in 1-D stimulated ESEEM which arises from the τ-dependent amplitude of the nuclear coherences excited by the $\pi/2$—τ—$\pi/2$ subsequence. This latter effect has been shown to occur also when $I > \frac{1}{2}$.

The results of the earlier first-order analysis have been reproduced by omitting the nonlinear terms, an approximation possible only when $k \cong 0$. The general theory allows one to know the error caused by the neglect of high-order terms and then the suitability of the older theory to specific situations. Such error is reasonably small for $I = 1$ nuclei such as deuterium even at rather large k, but it becomes so large for high-spin nuclei that the earlier analysis does not apply properly even at small k. It is then clear that the general theory permits a more thorough understanding of the ESEEM from high-spin nuclei (provided that they are not subject to a large nuclear quadrupole interaction), which have not been routinely studied by ESEEM spectroscopy up to now. The present treatment also reveals the usefulness of performing experiments at different k values when $I > \frac{1}{2}$ nuclei are involved. The modulation depth parameter can be experimentally affected by a change in the strength of the nuclear Zeeman interaction (or by sample rotation for ordered systems). This can be in general achieved by using a different microwave frequency or, in a more limited manner, by exciting at different magnetic field settings when the sample exhibits anisotropy. The modulation amplitude vs k plots provide a useful tool to predict the effect of changing k on the spectrum and then to design a strategy suited to the experimenter's goals. At variance with the first-order theory, which suggests making k as large as possible to gain sensitivity, it is now recognized that a larger k usually yields a lower resolution due to an increased number of spectral lines and may even result in lower sensitivity if the maximum amplitude point is at smaller k. For instance, as the fundamental modulations have large amplitude and dominate the spectrum when the modulation depth parameter is small (especially for large I), in order to improve resolution one could prefer a small k when performing ESEEM experiments on samples containing high-spin nuclei. This peculiar behavior makes the direct measurement of the principal values of the hyperfine interaction in principle feasible: since k is always small near the hyperfine principal directions, one can choose an excitation frequency such that the amplitude of the fundamental modulations from centers oriented close to the principal directions is preferentially enhanced. For ordered systems, this means that spectral lines closely related to the hyperfine principal values have significant amplitude; in disordered systems, the ''turning points'' typical of CW-ENDOR can be recovered. Another useful tool is provided by putting the suppression effect in 1-D stimulated ESEEM to good use. When $I > \frac{1}{2}$, one can choose τ in the vicinity of a blind spot to preferentially suppress higher harmonics, another example of trading sensitivity for resolution. Finally, on the basis of the reported theory, a very efficient algorithm for the simulation of ESEEM spectra has been designed and implemented which features a reduction of the computing time by about three orders of magnitude compared to existing procedures.

REFERENCES

1. A. Schweiger, *Appl. Magn. Reson.* **5,** 229 (1993).
2. W. B. Mims, K. Nassau, and J. D. McGee, *Phys. Rev.* **123,** 2059 (1961).
3. L. G. Rowan, E. L. Hahn, and W. B. Mims, *Phys. Rev.* **137,** 61 (1965).
4. W. B. Mims, *Phys. Rev. B* **5,** 2409 (1972); W. B. Mims, *Phys. Rev. B* **6,** 3543 (1972).
5. W. B. Mims, J. Peisach, and J. L. Davis, *J. Chem. Phys.* **66,** 5536 (1977).
6. A. A. Shubin and S. A. Dikanov, *J. Magn. Reson.* **52,** 1 (1983).
7. M. Romanelli, M. Narayana, and L. Kevan, *J. Chem. Phys.* **80,** 4044 (1984).
8. T. Ichikawa, *J. Chem. Phys.* **83,** 3790 (1985).
9. M. K. Bowman and R. J. Massoth, *in* ''Electronic Magnetic Resonance in the Solid State'' (J. A. Weil, M. K. Bowman, J. R. Morton, and K. F. Preston, Eds.), p. 99, Can. Soc. Chem., Ottawa, 1987.
10. K. Matar and D. Goldfarb, *J. Chem. Phys.* **96,** 6464 (1992).
11. K. Matar and D. Goldfarb, *J. Magn. Reson. A* **111,** 50 (1994).

12. A. Schweiger, C. Gemperle, and R. R. Ernst, *J. Magn. Reson.* **86,** 70 (1990); E. J. Hustedt, A. Schweiger, and R. R. Ernst, *J. Chem. Phys.* **96,** 4954 (1992); J. Sebbach, E. C. Hoffmann, and A. Schweiger, *J. Magn. Reson. A* **116,** 221 (1995).
13. M. K. Bowman, *Isr. J. Chem.* **32,** 339 (1992); E. C. Hoffmann and A. Schweiger, *Chem. Phys. Lett.* **220,** 467 (1994); E. C. Hoffmann, M. Hubrich, and A. Schweiger, *J. Magn. Reson. A* **117,** 16 (1995).
14. G. Jeschke and A. Schweiger, *Molec. Phys.* **88,** 355 (1996); G. Jeschke and A. Schweiger, *J. Chem. Phys.* **105,** 2199 (1996).
15. S. A. Dikanov, A. A. Shubin, and V. N. Parmon, *J. Magn. Reson.* **42,** 474 (1981).
16. (*a*) D. Goldfarb and L. Kevan, *J. Am. Chem. Soc.,* **109,** 2303 (1987); (*b*) A. Tyryshkin, S. A. Dikanov, and E. J. Reijerse, *J. Magn. Reson. A* **116,** 10 (1995).
17. R. P. Merks and R. de Beer, *J. Magn. Reson.* **37,** 305 (1980).
18. J. Isoya, M. K. Bowman, J. R. Norris, and J. A. Weil, *J. Chem. Phys.* **78,** 1735 (1983).
19. X. Tan, M. Bernardo, H. Thomann, and C. P. Scholes, *J. Chem. Phys.* **102,** 2675 (1995).
20. H. Barkhuijsen, R. de Beer, E. L. de Wild, and D. van Ormondt, *J. Magn. Reson.* **50,** 299 (1982).
21. L. Kevan, *in* ''Time Domain Electron Spin Resonance'' (L. Kevan and R. N. Schwartz, Eds.), Chap. 8, Wiley, New York, 1979.
22. A. Schweiger, *in* ''Modern Pulsed and Continuous-Wave Electron Spin Resonance'' (L. Kevan and M. K. Bowman, Eds.), Chap. 2, Wiley, New York, 1990.
23. R. R. Ernst, G. Bodenhausen, and A. Wokaun, ''Principles of Magnetic Resonance in One and Two Dimensions,'' Chap. 2, Clarendon Press, Oxford, 1991.
24. A. Ponti and A. Schweiger, *Appl. Magn. Reson.* **7,** 363 (1994).
25. E. P. Wigner, ''Group Theory and Its Application to the Quantum Mechanics of Atomic Spectra,'' Chaps. 14 and 15, Academic Press, New York, 1959.
26. M. Tinkham, ''Group Theory and Quantum Mechanics,'' Chap. 5, McGraw–Hill, New York, 1964.
27. G. Arfken, ''Mathematical Methods for Physicists,'' Chap. 13, Academic Press, New York, 1985.
28. U. W. Hochstrasser, *in* ''Handbook of Mathematical Functions'' (M. Abramowitz and I. A. Stegun, Eds.), Dover, New York, 1965.
29. J.-M. Fauth, A. Schweiger, L. Braunschweiler, J. Forrer, and R. R. Ernst, *J. Magn. Reson.* **66,** 74 (1986).
30. R. P. J. Merks and R. de Beer, *J. Chem. Phys.* **83,** 3319 (1979).
31. I. S. Gradshteyn and I. M. Ryzhik, ''Tables of Integrals, Series, and Products,'' p. 25, Academic Press, New York, 1980.
32. J. A. Weil, J. R. Bolton, and J. E. Wertz, ''Electron Paramagnetic Resonance,'' p. 534, Wiley, New York, 1994.
33. S. A. Smith, T. O. Levante, B. H. Meier, and R. R. Ernst, *J. Magn. Reson. A* **106,** 75 (1994).
34. P. Höfer, A. Grupp, H. Nebenführ, and M. Mehring, *Chem. Phys. Lett.* **132,** 279 (1986).
35. A. Ponti and A. Schweiger, *J. Chem. Phys.* **102,** 5207 (1995).
36. A. Schweiger, *Angew. Chem. Int. Ed. Engl.* **30,** 265 (1991).
37. M. Hubrich, G. Jeschke, and A. Schweiger, *J. Chem. Phys.* **104,** 2172 (1995).
38. P. Höfer, *J. Magn. Reson. A* **111,** 77 (1994).
39. Matlab Version 4.2c, The Mathworks, Inc., 1994.
40. L. Kevan, *in* ''Modern Pulsed and Continuous-Wave Electron Spin Resonance'' (L. Kevan and M. K. Bowman, Eds.), Chap. 5, Wiley, New York, 1990.
41. H. Cho, S. Pfenninger, C. Gemperle, A. Schweiger, and R. R. Ernst, *Chem. Phys. Lett.* **160,** 391 (1989).
42. J.-M. Fauth, A. Schweiger, and R. R. Ernst, *J. Magn. Reson.* **81,** 262 (1989).
43. A. Lai, H. L. Flanagan, and D. J. Singel, *J. Chem. Phys.* **89,** 7161 (1988).